

## Thermotropic and barotropic phase transitions on diacylphosphatidylethanolamine bilayer membranes

Hitoshi Matsuki<sup>1,\*</sup>, Shigeru Endo<sup>2</sup>, Ryosuke Sueyoshi<sup>2</sup>,  
Masaki Goto<sup>1</sup>, Nobutake Tamai<sup>1</sup> and Shoji Kaneshina<sup>2</sup>

<sup>1</sup>Graduate School of Bioscience and Bioindustry, Tokushima University, +  
2-1 Minamijosanjima-cho, Tokushima 770-8513, Japan

<sup>2</sup>Department of Biological Science and Technology, Faculty of Engineering,  
Tokushima University, 2-1 Minamijosanjima-cho, Tokushima 770-8506, Japan

Mailing address: Hitoshi Matsuki

Graduate School of Bioscience and Bioindustry

Tokushima University

2-1 Minamijosanjima-cho, Tokushima 770-8513, Japan

TEL: +81-88-656-7513

FAX: +81-88-655-3162

E-mail address: [matsuki@tokushima-u.ac.jp](mailto:matsuki@tokushima-u.ac.jp)

\*Corresponding author

## Abstract

The bilayer phase transitions of four diacylphosphatidylethanolamines (PEs) with matched saturated acyl chains ( $C_n = 12, 14, 16$  and  $18$ ) and two PEs with matched unsaturated acyl chains containing a different kind of double bonds were observed by differential scanning calorimetry under atmospheric pressure and light-transmittance measurements under high pressure. The temperature-pressure phase diagrams for these PE bilayer membranes were constructed from the obtained phase-transition data. The saturated PE bilayer membranes underwent two different phase transitions related to the liquid crystalline ( $L_\alpha$ ) phase, the transition from the hydrated crystalline ( $L_c$ ) phase and the chain melting (gel ( $L_\beta$ ) to  $L_\alpha$ ) transition, depending on the thermal history. Pressure altered the gel-phase stability of the bilayer membranes of PEs with longer chains at a low pressure. Comparing the thermodynamic quantities of the saturated PE bilayer membranes with those of diacylphosphatidylcholine (PC) bilayer membranes, the PE bilayer membranes showed higher phase-transition temperatures and formed more stable  $L_c$  phase, which originates from the strong interaction between polar head groups of PE molecules. On the other hand, the unsaturated PE bilayer membranes underwent the transition from the  $L_\alpha$  phase to the inverted hexagonal ( $H_{II}$ ) phase at a high temperature and this transition showed a small transition enthalpy but high-pressure responsivity. It turned out that the kind of double bonds markedly affects both bilayer-bilayer and bilayer-nonbilayer transitions and the  $L_\alpha/H_{II}$  transition is a volume driven transition for the reconstruction of molecular packing. Further, the phase-transition behavior was explained by chemical potential curves of bilayer phases.

*Key words:* Differential scanning calorimetry, Lipid bilayer membrane, Phase stability, Phase transition, Phosphatidylethanolamine, Pressure

## 1. Introduction

Glycerophospholipids are main constituent lipids in biological membranes. There are so many glycerophospholipids with different hydrophobic acyl chains and a different hydrophilic polar head group. Phosphatidylcholines (PCs) are widely distributed in biological membranes and the bilayer aggregates such as vesicles and liposomes formed by PC molecules in the aqueous solution are frequently used as model bio-membranes. PC bilayer membranes take several membrane states like gel and liquid crystalline phases depending on the orientation or packing of the PC molecules in the bilayer membrane. They vary between membrane states by structural changes called phase transitions. Reports on temperature induced structural changes, thermotropic phase transitions, of PC bilayer membranes have been made in large numbers [1-3], whereas those on pressure induced changes, barotropic phase transition, have been made in very limited numbers [4-14]. We focus our attention on the pressure effect of lipid bilayer membranes and have investigated the bilayer phase transitions of various kinds of PCs with different molecular structures such as chain length, chain unsaturation, chain asymmetry and linkage to a glycerol backbone [15-22]. Thereby, the phase transitions of these PC bilayer membranes depending temperature and pressure have been elucidated thermodynamically.

In addition to PC, there is another principal glycerophospholipid species, phosphatidylethanolamines (PEs). PE universally exists in biological membranes from prokaryotes like *Escherichia coli* to eukaryotes like mammals although PC does not in those of prokaryotes. PE has a small-sized polar head group, ethanolamine ( $-\text{CH}_2-\text{CH}_2-\text{N}^+\text{H}_3$ ) group, in contrast with PC with a large-sized head group, choline ( $-\text{CH}_2-\text{CH}_2-\text{N}^+(\text{CH}_3)_3$ ) group. It has been reported that bilayer membranes formed by PEs with saturated fatty acids as acyl chains, which we call saturated PEs here, exhibit gel and liquid crystalline phases similar to those formed by PCs with the same chains, but the membrane states are considerably different from each other [23-34]. On the other hand, PEs with unsaturated

fatty acids as acyl chains, which we call unsaturated PEs here, form one of nonbilayer phases called an inverted hexagonal phase at higher temperatures beyond the temperature range of the liquid crystalline phase [35-46], the structure of which can not be formed in PC bilayer membranes. It is considered that the inverted hexagonal structure is partially and transiently formed in various cell or organelle membranes and plays an important role as local and transitional intermediates in cellular process related to morphological changes of membranes such as membrane fusion and fission, membrane transport as exo- and endocytosis [45,47-49].

There are many reports on thermotropic phase transitions of PE bilayer membranes though, barotropic phase-transition data are quite lacking and only a few data concerning the pressure effect on the bilayer phase transition of certain PEs have been reported by some groups including us [4,46,50-52]. Hence, the systematic study of the pressure effect on PE bilayer membranes remains to be investigated. In the present study, for the purpose of examining of the phase transitions for the PE bilayer membranes under high pressure, we selected four diacylphosphatidylethanolamines (PEs) with matched saturated acyl chains, dilauroylphosphatidylethanolamine (12:0-PE), dimyristoylphosphatidylethanolamine (14:0-PE), dipalmitoylphosphatidylethanolamine (16:0-PE) and distearoylphosphatidylethanolamine (18:0-PE), and two PEs with matched unsaturated acyl chains containing a different kind of double bonds, dioleoylphosphatidylethanolamine (18:1(*cis*)-PE) and dielaidoylphosphatidylethanolamine (18:1(*trans*)-PE). The phase transitions of these PE bilayer membranes were observed as a function of temperature and pressure by differential scanning calorimetry (DSC) and high-pressure light transmittance measurement. By using the phase-transition data obtained, the thermotropic and barotropic phase transitions of the PE bilayer membranes are characterized from the temperature-pressure phase diagrams and the thermodynamic quantities of phase transitions. Furthermore, comparing the above results with the corresponding results of PCs with the same acyl chains as PEs [16,17,22], the resemblance and difference in phase transitions between PE and PC bilayer membranes are also discussed.

## 2. Experimental

### 2.1. Materials and sample preparation

Four synthetic phosphatidylethanolamines with different linear saturated acyl chains, 12:0-PE (1,2-didodecanoyl-*sn*-glycero-3-phosphoethanolamine), 14:0-PE (1,2-ditetradecanoyl-*sn*-glycero-3-phosphoethanolamine), 16:0-PE (1,2-dihexadecanoyl-*sn*-glycero-3-phosphoethanolamine) and 18:0-PE (1,2-dioctadecanoyl-*sn*-glycero-3-phosphoethanolamine), and two of them with different kinds of unsaturated acyl chains, 18:1(*cis*)-PE (1,2-di[*cis*-9-octadecenoyl]-*sn*-glycero-3-phosphoethanolamine) and 18:1(*trans*)-PE (1,2-di[*trans*-9-octadecenoyl]-*sn*-glycero-3-phosphoethanolamine), were respectively purchased from Avanti Polar Lipids, Inc. (Alabaster, AL). They were directly used without further purification. Ligroin (petroleum fraction consisting mostly of C<sub>7</sub> and C<sub>8</sub> hydrocarbons: Kanto Chemical Co., Inc., Japan) was used as a pressure-medium. Water was distilled twice after a deionization, where the second step was done from dilute alkaline permanganate solution.

The multilamellar vesicle dispersions were prepared by suspending each PE in water using a vortex mixer at a concentration of 1.0 mmol kg<sup>-1</sup> for PEs with saturated acyl chains and at a concentration of 5.0 mmol kg<sup>-1</sup> for PEs with unsaturated acyl chains. They were sonicated for a few minutes by using a Branson model 185 sonifier at a temperature several degrees above the L<sub>β</sub>/L<sub>α</sub>-transition temperature of each lipid. And then, the dispersions were allowed to stand at about -20 °C for at least 24 hours to form the hydrated crystalline phase. For the 16:0-PE and 18:0-PE bilayer membranes, a special pretreatment called thermal annealing was made because it is difficult to induce the hydrated crystalline phase in bilayer membranes of phospholipids with long saturated acyl chains [22,53,54]. Both PE dispersions were annealed by seven thermal cycles, where 1 thermal cycle comprises high-

temperature storage at 60°C (16:0-PE) or 70°C (18:0-PE) for one hour, and freezing storage at -15°C for more than 12 hours. All PE dispersions were sonicated again in a very short time at a designated temperature to adjust the multilamellar vesicle suitable for phase-transition observation of each lipid before experiments.

## *2.2. DSC measurements*

The phase transitions of PE bilayer membranes under atmospheric pressure were observed by use of high-sensitivity differential scanning calorimeters, MCS-DSC (MicroCal, Northampton, MA, USA) and VP-DSC (Malvern Instrum. Ltd., Worcestershire, UK). After a degas treatment of 10 – 15 minutes for sample and reference solutions, the measurements were started with a heating rate of 0.75 K min<sup>-1</sup>. The endothermic peaks in the DSC thermograms were analyzed by use of software Origin 7.0 (Lightstone Corp., Tokyo, Japan). DSC measurements of the 18:1(*cis*)-PE bilayer membrane at low temperatures below the freezing point of water were also performed by using a SSC 5200-DSC 120 calorimeter (SII Nanotechnology Co. Ltd, Chiba, Japan). The prepared sample and reference solutions were sealed up to the amount of 60 µl in DSC silver cells. After reaching thermal equilibrium, the measurements were carried out under a heating rate of 0.3 or 0.5 K min<sup>-1</sup>. The endothermic peaks were analyzed by attached software for the apparatus. The thermal quantities were averaged with the standard deviations from at least triplicate measurements.

## *2.3. High-pressure light transmittance measurements*

Since the refractive index of a dilute vesicle solution noticeably changes at a phase transition, we adopted light-transmittance measurements as the phase-transition experiments under high pressure. The phase transitions under high pressure were observed by a light transmittance technique using a high-pressure cell assembly PCI-400 (or PCI-500) (Syn.

Corp., Kyoto, Japan) attached to U-3010 (or U-3900) spectrophotometer (Hitachi High-Technology Corp., Tokyo, Japan). Two kinds of light-transmittance measurements developed in our laboratory were made; one is an isobaric thermotropic observation by scanning temperature at constant pressure and the other is an isothermal barotropic observation by scanning pressure at constant temperature. Pressures were generated by a hand-operated HP-500 hydraulic pump (Syn. Corp., Kyoto, Japan) and monitored using a Heise gauge with an accuracy of 0.2 MPa. Temperature of the pressure cell was controlled by circulating thermostated water from a water bath through a jacket enclosing the cell. Abrupt changes in transmittance of monochromic light (wavelength 560 nm) were observed at phase transitions and the phase-transition temperatures or pressures were determined from the inflection points in the transmittance vs. temperature or pressure curve. The heating rate at a given pressure in the isobaric thermotropic measurements and the pressurizing rate at a given temperature were  $0.5 \text{ K min}^{-1}$  and 20 MPa (5 MPa in the vicinity of the phase transition) with a 15-min interval, respectively. The measurements were performed in at least triplicate under the isobaric or isothermal conditions. The detailed procedures for the light transmittance measurements were described elsewhere [15,17,20].

### **3. Results**

#### *3.1. Thermal behavior of diacyl-PE bilayer membranes under atmospheric pressure*

The DSC thermograms of all diacyl-PE bilayer membranes in a heating scan are presented in Fig. 1. We observed two kinds of endothermic peaks depending on the thermal history of a lipid sample in the thermograms of the saturated PE bilayer membranes. One large endothermic peak was obtained in the first heating scan after freezing storage. But in the subsequent scan (second scan), which was reheated immediately after cooling the lipid sample, another endothermic peak that is smaller than the peak in the first scan appeared in

the different temperature range from the first scan. With increasing acyl chain length, the peak temperatures of both scans increased and the difference in temperature between both scans decreased. For the 18:0-PE bilayer membrane, we could not observe two endothermic peaks depending on the thermal history but only low-temperature transition in both scans by a usual thermal annealing repeating freeze ( $-15^{\circ}\text{C}$ ) and thaw ( $5^{\circ}\text{C}$ ) cycles. However, by using a special annealing described in the experimental section, we could detect two kinds of peaks similar to those of other three saturated PE bilayer membranes. It was reported in the 12:0-PE and 14:0-PE bilayer membranes [27-33] that the phase states are influenced by the thermal history of a lipid sample and they undergo a phase transition from the subgel or hydrated crystalline ( $L_c$ ) phase to the liquid crystalline ( $L_{\alpha}$ ) phase and a phase transition from the gel ( $L_{\beta}$ ) phase to the  $L_{\alpha}$  phase because the rate of transformation into the  $L_c$  phase is slow. We assigned the higher-temperature transition obtained by the first scan as the  $L_c/L_{\alpha}$  transition while the lower-temperature transition obtained by the second scan as the  $L_{\beta}/L_{\alpha}$  transition. Although the saturated PE bilayer membranes are known to exhibit a metastable  $L_c$  phase depending on the thermal history of a lipid sample [55, 56], we addressed only the phase transition from the stable  $L_c$  phase in this study. The temperatures of the  $L_c/L_{\alpha}$  and  $L_{\beta}/L_{\alpha}$  transitions except for the  $L_c/L_{\alpha}$  transition of the 18:0-PE bilayer membrane were in good agreement with those in the tables constructed by Koynova and Caffrey [1,34].

In the DSC thermograms of the unsaturated PE bilayer membranes, we also observed endothermic peaks at two temperatures for both PE bilayer membranes, but the behavior was not sensitive to thermal history unlike the saturated PEs. A relatively large endothermic peak was obtained for both PE bilayer membranes in the different temperature range: at a low temperature around  $-5^{\circ}\text{C}$  for the 18:1(*cis*)-PE bilayer membrane and at a high temperature about  $38^{\circ}\text{C}$  for the 18:1(*trans*)-PE bilayer membrane. Generally, one relatively large transition found for an unsaturated lipid bilayer membrane has been regarded as a chain melting ( $L_{\beta}/L_{\alpha}$ ) transition, and the transitions observed for both PE bilayer membranes have been assigned as the  $L_{\beta}/L_{\alpha}$  transition [1,34,57]. However, the special attention must be taken



in treating a phase transition at a temperature below 0°C (freezing point of water) due to the acceleration of the  $L_c$ -phase formation. We recently analyzed the transition of the 18:1(*cis*)-PE bilayer membrane and identified the transition as the  $L_c/L_\alpha$  transition not the  $L_\beta/L_\alpha$  transition [50]. The  $L_\beta$  phase of the 18:1(*cis*)-PE bilayer membrane may be unstable at temperatures below 0°C and could not be observed in this study. As for the 18:1(*trans*)-PE bilayer membrane, this transition is the  $L_\beta/L_\alpha$  transition itself as will be shown later. On the other hand, there existed another small endothermic peak in the thermograms of both PE bilayer membranes [35-37]. Unsaturated PE bilayer membranes are known to form an inverted hexagonal structure at high temperatures above the  $L_\beta/L_\alpha$ -transition temperature. We identified the small peak observed in the high temperature region as the transition from the  $L_\alpha$  phase to the inverted hexagonal ( $H_{II}$ ) phase. The temperatures were in fair agreement with those reported in literatures [34,42,44].

### *3.2. Phase transitions of diacyl-PE bilayer membranes under high pressure*

Figure 2 depicts examples of light-transmittance curves of several PE (14:0-PE, 18:0-PE and 18:1(*trans*)-PE) bilayer membranes measured by the method of isobaric thermotropic observation under atmospheric and high pressure. An abrupt change in the transmittance vs. temperature curves was found for the saturated PE bilayer membranes depending on the thermal history under atmospheric pressure, that is, the  $L_c/L_\alpha$  transition in the first scan and the  $L_\beta/L_\alpha$  transition in the second scan. The phase-transition temperatures determined from the transmittance changes were in almost accord with those obtained by DSC (e.g. Fig. 2(a) for the 14:0-PE bilayer membrane). The transmittance vs. temperature curves of the 12:0-PE and 14:0-PE bilayer membranes under high pressure exhibited the similar thermally historic behavior to those under atmospheric pressure and the transition temperatures were elevated by applying pressure. In the 16:0-PE and 18:0-PE bilayer membranes under high pressure, we found two-step transitions in the first scan but a single-step transition in the

second scan (Fig. 2(b) for the 18:0-PE bilayer membrane) [50,51,58], although all phase-transition temperatures increased by applying pressure. Since the temperature of the  $L_{\beta}/L_{\alpha}$  transition in the second scan coincided with that of the latter transition in the first scan, two transitions observed in the first scan were assigned as the  $L_c/L_{\beta}$  and  $L_{\beta}/L_{\alpha}$  transitions, respectively. Here it should be noted in the both bilayer membranes that the  $L_{\beta}/L_{\alpha}$  transition can be observed at a temperature higher than the  $L_c/L_{\beta}$ -transition temperature.

Abrupt changes in the transmittance vs. temperature curves were also found for the unsaturated PE bilayer membranes. The temperature shift of both  $L_{\beta}/L_{\alpha}$  and  $L_{\alpha}/H_{II}$  transitions to the high-temperature region on the transmittance curves of the 18:1(*trans*)-PE bilayer membrane by applying pressure was always detected with high accuracy (Fig. 2(c)). For the 18:1(*cis*)-PE bilayer membrane, the  $L_c/L_{\alpha}$  transition could be only observed on the transmittance curves under high pressure due to the freezing of solvent water under atmospheric pressure, whereas the  $L_{\alpha}/H_{II}$  transition could be clearly observed on the transmittance curves under atmospheric and high pressure irrespective of the thermal history (data not shown).

### 3.3. Phase diagrams of diacyl-PE bilayer membranes

We determined the phase-transition temperatures of all diacyl-PE bilayer membranes under atmospheric pressure from the DSC measurements as given in Fig. 1, those under high pressure from the isobaric thermotropic transmittance measurements as given in Fig. 2 and the phase-transition pressures under constant temperature from the isothermal barotropic transmittance measurements (data not shown). Now we can construct the temperature ( $T$ )-pressure ( $p$ ) phase diagram of each diacyl-PE bilayer membrane. The resulting  $T$ - $p$  phase diagrams of six diacyl-PE bilayer membranes are demonstrated in Figs. 3 and 4, respectively. We immediately notice from the phase diagrams in Fig. 3 that the phase diagrams of the 12:0-PE and 14:0-PE bilayer membranes and those of the 16:0-PE and 18:0-PE bilayer membranes

are different. In the 12:0-PE and 14:0-PE bilayer membranes, the temperatures of the  $L_c/L_\alpha$  and  $L_\beta/L_\alpha$  transitions increased by applying pressure and the  $T$ - $p$  curves of both transitions were convex upward slightly. The  $L_c/L_\alpha$  transition was always located above the  $L_\beta/L_\alpha$  transition in the diagrams, and the temperature difference between both transitions became narrower in the high-pressure region because the pressure dependence of transition temperature ( $dT/dp$ ) was slightly greater in the  $L_\beta/L_\alpha$  transition ( $0.23 - 0.25 \text{ K MPa}^{-1}$ ) than that in the  $L_c/L_\alpha$  transition ( $0.21 - 0.22 \text{ K MPa}^{-1}$ ). In contrast to the above phase behavior, two transition curves intersected with each other at a relatively low pressure in the 16:0-PE and 18:0-PE bilayer membranes. The pressures and temperatures of the intersection point for the 16:0-PE and 18:0-PE bilayer membranes were obtained as 22 MPa and 69°C, 14 MPa and 78°C, respectively. At pressures below the intersection pressure, either  $L_c/L_\alpha$  transition or  $L_\beta/L_\alpha$  transitions was observed in accordance with the thermal hysteresis, whereas at high pressures above the intersection pressure, the  $L_c/L_\beta$  transition, not the  $L_c/L_\alpha$  transition, and  $L_\beta/L_\alpha$  transitions were observed consecutively. Thus, we can say that the phase stability of the  $L_\beta$  phase changes at the intersection point, that is, the phase changes from metastable to stable at the point. The systematic change in the phase behavior for the saturated PE bilayer membrane depending on the chain length is attributable to the fact that the elevation of the transition temperature accompanied with the chain elongation is larger for the  $L_\beta/L_\alpha$  transition in comparison with the transition related to the  $L_c$  phase ( $L_c/L_\alpha$  or  $L_c/L_\beta$  transition). Furthermore, unlike the case of bilayer membranes of PCs with saturated acyl chains, the gel-phase polymorphism and new pressure-induced phase such as an interdigitated gel ( $L_\beta\text{I}$ ) phase [8,10,17,22] were not found in the bilayer membranes of PEs with the same acyl chains as PCs at all.

The phase diagrams of the unsaturated PE bilayer membranes (Fig. 4) exhibited remarkably different behavior from those of the saturated PE bilayer membranes (Fig. 3). All phase-transition temperatures were also elevated by applying pressure, but the degree of the temperature elevation for each transition was different. The  $dT/dp$  value of the  $L_c/L_\alpha$

transition for the 18:1(*cis*)-PE bilayer membrane (0.146 K MPa<sup>-1</sup>) and that of the L<sub>β</sub>/L<sub>α</sub> transition for the 18:1(*trans*)-PE bilayer membrane (0.209 K MPa<sup>-1</sup>) were smaller than those of the corresponding transitions for the saturated PE bilayer membranes. Here, it should be noted that the  $dT/dp$  value of the L<sub>α</sub>/H<sub>II</sub> transition for the 18:1(*cis*)-PE bilayer membrane (0.391 K MPa<sup>-1</sup>) was the largest of all phase transitions observed in phospholipid bilayer membranes, in other word, this transition was the most responsive to pressure. This largest value was in good agreement with that reported by Winter et al. [52]. Whereas, in the L<sub>α</sub>/H<sub>II</sub> transition for the 18:1(*trans*)-PE bilayer membrane, the  $dT/dp$  value (0.250 K MPa<sup>-1</sup>) was considerably smaller than that of the 18:1(*cis*)-PE bilayer membrane. We have elucidated in previous phase-transition studies of phospholipid bilayer membranes [17,19-22,59] that the  $dT/dp$  values of bilayer membranes for phospholipids with acyl- or alkyl-chain homologs have similar values if their transitions are the same kinds of transitions as one another. However, the present results indicated that the tendency is not applicable in bilayer membranes of PEs with unsaturated chains of geometrical isomers. Concerning the L<sub>α</sub>/H<sub>II</sub> transition for the saturated PE bilayer membranes, since it is reported that the transition temperatures locate at temperatures higher than the boiling point of water [3,33,39,40], we could not observe the transition in the saturated PE bilayer membranes but observe the transition in the unsaturated PE bilayers because of the large transition-temperature reduction by introducing a double bond into acyl chains of the molecule [18,58].

#### 4. Discussion

The thermodynamic quantities associated with the phase transitions under atmospheric pressure, the enthalpy ( $\Delta H$ ), entropy ( $\Delta S$ ) and volume ( $\Delta V$ ) changes, were evaluated from the phase-transition experiments. The  $\Delta H$  values were determined from the peak areas given in Fig. 1, and the  $\Delta S$  values were obtained by using the relation held at phase equilibrium:

$$\Delta S = \Delta H/T. \quad (1)$$

The  $\Delta V$  values were estimated by applying the following Clapeyron equation

$$\Delta V = \Delta H(dT/dp)/T \quad (2)$$

to the transition-temperature ( $T$ ) and  $\Delta H$  values and the  $dT/dp$  value that obtained from the  $T$  vs.  $p$  curve under atmospheric pressure in Figs. 3 and 4. The resulting thermodynamic quantities are summarized together with the  $T$  and  $dT/dp$  values in Table 1 for the saturated PE bilayer membranes and those in Table 2 for the unsaturated PE bilayer membranes, respectively. In Table 1, are also included the apparent  $\Delta V$  values of the  $L_c/L_\beta$  transition for the 16:0-PE and 18:0-PE bilayer membranes, which were calculated by using the difference in  $\Delta H$  values between  $L_c/L_\alpha$  and  $L_\beta/L_\alpha$  transitions with  $T$  and  $dT/dp$  values at a high pressure under the assumption that the pressure effect on  $\Delta H$  is negligible at a pressure of the intersection point. The calculated  $\Delta V$  values of the  $L_c/L_\beta$  transition were almost comparable to those obtained from the difference in  $\Delta V$  values between  $L_c/L_\alpha$  and  $L_\beta/L_\alpha$  transitions. The agreement of both values thermodynamically supports that the phase transition induced by pressure is exactly the  $L_c/L_\beta$  transition.

#### *4.1. Thermodynamic properties for phase transitions of saturated diacyl-PE bilayer membranes*

Figure 5 shows the chain-length dependence of the  $L_c/L_\alpha$ -transition and  $L_\beta/L_\alpha$ -transition temperatures for the saturated PE bilayer membranes. Both transition temperatures increased with increasing acyl chain length but the shape of the curves was different: the curve was nearly linear for the  $L_c/L_\alpha$  transition while it was convex upward for the  $L_\beta/L_\alpha$  transition. The temperature difference between both transitions became narrower with the chain elongation, and both transition curves almost coincided with each other at chain length of 18. Judging from the chain-length dependence of both transition curves, we expect that the intersection point of both transition curves might be observed if the temperature data could be extrapolated to longer chain length. And the behavior of the chain-length

dependence of both transition curves is qualitatively similar to that of the pressure dependence of both curves given in Fig. 3. This fact means that the increase in cohesive force due to a van der Waals interaction in saturated PE bilayer membranes brings the similar change in bilayer phase behavior to the case of pressure. In Fig. 5, are also given the temperatures of the gel/ $L_\alpha$ -transition (correctly,  $P_\beta'/L_\alpha$  transition) and those of the transitions related to the  $L_c$  phase ( $L_c$ /gel transition, see below) for bilayer membranes of the corresponding PCs (12:0-PC, 14:0-PC, 16:0-PC and 18:0-PC) with the same acyl chains as PEs [17,22,60]. In comparison with bilayer membranes of the PE and PC series, the temperatures of the gel/ $L_\alpha$  transition for the PE series were about 19 – 33 K higher than those for the PC series and the temperatures of the  $L_c$ / $L_\alpha$  transition for the PE series were 43 – 45 K higher than those of the  $L_c$ /gel transition for the PC series. Remarkable difference in both transition temperatures between PE and PC series is attributable to the difference in structure between their polar head groups. One PE molecule in the bilayer membrane can form the hydrogen bonding between a hydrogen atom bound to a nitrogen atom quaternalized in an ethanolamine group and an oxygen atom of a phosphate group in an adjacent PE molecule, and hence the interaction between polar head groups is strengthened [61-63]. The existence of hydrogen bonding in condensed states such as the  $L_c$  and gel phases produces the great temperature elevation. Moreover, in addition to the strong interaction between the PE head groups, the small-sized head group enables two acyl chains to orient perpendicularly from the membrane surface due to the least steric hindrance for the molecular conformation, and then the PE molecules do not need to tilt to accommodate the difference between head group and chain cross-sectional area, so only one gel phase is observed. This behavior contrasts with the fact that the large-sized choline head group makes the acyl chains tilt from the membrane surface by about 30°, the large steric hindrance of which is responsible for the gel-phase polymorphism of the PC bilayer membranes.

The chain-length dependence of  $\Delta H$  and  $\Delta V$  values of the  $L_c/L_\alpha$  transition and  $L_\beta/L_\alpha$  transition for the saturated PE bilayer membranes is depicted in Fig. 6. The  $\Delta H$  and  $\Delta V$

values of the  $L_c/L_\alpha$  transition and  $L_\beta/L_\alpha$  transition increased with increasing acyl chain length and both values of the  $L_c/L_\alpha$  transition were about two or three times larger than those of the  $L_\beta/L_\alpha$  transition. The  $L_\beta/L_\alpha$  transition results from *trans-gauche* conformational changes of lipid molecules in the bilayer membranes, that is, a phenomenon of acyl chain melting. On the other hand, the  $L_c/L_\alpha$  transition is the direct transformation from the  $L_c$  phase to the  $L_\alpha$  phase. It contains the mobility change in hydrophobic acyl chains and the hydration change near a hydrophilic ethanolamine head group in addition to the process of the chain melting. The  $\Delta H$  and  $\Delta V$  values of the  $L_c/L_\beta$  transition, which can be obtained by subtracting the values of the  $L_\beta/L_\alpha$  transition from those of the  $L_c/L_\alpha$  transition respectively, were considerably larger compared with those of the  $L_\beta/L_\alpha$  transition. This fact is quite different from the case of the saturated PC bilayer membranes, which will be compared below, and means that the saturated PE bilayer membranes form the significantly stable  $L_c$  phase.

The  $\Delta H$  values of the  $L_c/L_\alpha$  transition and  $L_\beta/L_\alpha$  transition for the saturated PE bilayer membranes have been compiled with several literatures by Koynova, et al. [34] and also obtained from DSC with high accuracy by Lewis, et al. [33]. Our  $\Delta H$  values for the  $L_c/L_\alpha$  transition were the highest of the three data: they were considerably larger than those of Koynova, et al. and relatively close to those for Lewis, et al. although the latter data were only obtained for the 12:0-PE and 14:0-PE bilayer membranes. For the  $\Delta V$  values, Koynova, et al. [31] have determined them by densitometry. Our results for the  $L_\beta/L_\alpha$  transition were almost comparable with these data, whereas those for the  $L_c/L_\alpha$  transition were different among them. They showed almost the same  $\Delta V$  values of the  $L_c/L_\alpha$  transition for the saturated PE bilayer membranes irrespective of the acyl chain length. However, our results indicated definite acyl chain length dependence as well as the case of the  $L_\beta/L_\alpha$  transition. We speculate that the difference in  $\Delta H$  and  $\Delta V$  values of the  $L_c/L_\alpha$  transition may be caused by the difference in lipid sample preparation. In this study, we performed thermal annealing on samples of long chain PEs for the  $L_c$ -phase observation and thereby we observed the  $L_c/L_\alpha$  transition for all saturated PE bilayer membranes. Taking into account that the  $L_c/L_\alpha$  transition includes the

chain melting and the  $\Delta H$  and  $\Delta V$  values of subtransition for the saturated PC bilayer membranes also exhibit the definite chain length dependence [22], it can be said that the present values are reasonable for those of the transition from the  $L_c$  phase formed completely to the  $L_\alpha$  phase.

#### *4.2. Comparison of phase-transition enthalpies and volumes between saturated diacyl-PE and diacyl-PC bilayer membranes*

The  $\Delta H$  and  $\Delta V$  values of bilayer membranes of the PC series are also compared in Fig. 6. Here, since PC bilayer membranes exhibit the gel-phase polymorphism such as the lamellar gel ( $L_\beta'$ ) and ripple gel ( $P_\beta'$ ) phases with tilted lipid molecules, we used the values of the  $P_\beta'/L_\alpha$  transition as those of the  $gel/L_\alpha$  transition, and the cumulative values of the sub ( $L_c/L_\beta'$  or  $L_c/P_\beta'$ ), pre ( $L_\beta'/P_\beta'$ ) and main ( $P_\beta'/L_\alpha$ ) transitions as those of the  $L_c/L_\alpha$  transition except for the 12:0-PC bilayer membrane [17,22]. In the 12:0-PC bilayer membrane, the cumulative values of the  $L_c$ /(intermediate liquid crystalline:  $L_x$ ) and  $L_x/L_\alpha$  transitions in the 50% ethylene glycol solution were used as those of the  $L_c/L_\alpha$  transition [60]. Regarding the quantities of the  $gel/L_\alpha$  transition, the  $\Delta H$  and  $\Delta V$  values of both PE and PC series had the almost the same values as each other except for the bilayer membranes of chain length of 12. Resemblance of the quantities of the  $gel/L_\alpha$  transition for both PE and PC series reveals that the acyl chain melting is principally dependent on the chain length of a lipid molecule irrespective of the head-group structure. The results of  $\Delta H$  and  $\Delta V$  values for the PE and PC series form a striking contrast to the large difference in the  $gel/L_\alpha$ -transition temperature between both series given in Fig. 5.

Unlike the quantities of the  $gel/L_\alpha$ -transition, those of the  $L_c/L_\alpha$  transition for the PE series were larger than those for the PC series. Since the  $\Delta H$  and  $\Delta V$  values of the  $gel/L_\alpha$  transition for both PE and PC series were comparable to each other, it turned out that both values of the  $L_c/L_\beta$  transition for the PE series, which can be obtained from the difference



between the values of the  $L_c/L_\alpha$  and  $L_\beta/L_\alpha$  transitions, were larger than those for the PC series. This finding means that the difference between the  $L_c$  and  $L_\beta$  phases of the PE bilayer membrane is larger than the corresponding difference of the PC bilayer membrane. Results of X-ray diffraction measurements indicated that the molecular packing of the  $L_c$  phase is so tight that the state is nearly a solid crystalline state of a lipid [64-66]. Kodama et al. [67-70] took notice of the behavior of interlamellar water existing between lipid bilayer membranes and revealed the difference in hydration structure between the  $L_c$  and  $L_\beta$  phases by applying a DSC method detecting ice-melting peaks to lipid-water systems with various water contents. According to their results, a 16:0-PC molecule in the  $L_\beta$  (exactly  $L_\beta'$ ) phase of the bilayer membrane has 10 interlamellar (5 nonfreezable and 5 freezable) water molecules, whereas a 14:0-PE molecule in the bilayer membrane has 6 (2.3 nonfreezable and 3.7 freezable) ones. When converting from the  $L_\beta$  phase to the  $L_c$  phase, the total number of interlamellar water molecules for the 16:0-PC molecule does not change although the ratio of nonfreezable and freezable water molecules changes from 5:5 to 6:4. On the contrary, the 14:0-PE molecule in the  $L_c$  phase releases about 5 interlamellar water molecules into bulk water phase and then has only 1.3 interlamellar (0.3 nonfreezable and 1 freezable) water molecule, indicating that the ease with which interlamellar water molecules are released may be closely related to the stability of the  $L_c$  phase. The stronger stability of the  $L_c$  phase of PE bilayer membrane than PC bilayer membrane is well correlated with the difference in hydration between PE and PC molecules in the bilayer membranes.

Furthermore, the difference in  $\Delta V$  value of the  $L_c/L_\alpha$  transition between PE and PC series became smaller with an increase in chain length in contrast with the difference in  $\Delta H$  value. This is attributable to the fact that the  $dT/dp$  values of the transition related to the  $L_c$  phase for short chain PC bilayer membranes are considerably small in comparison with the corresponding PE series. In the bilayer membranes of chain length of 18, the  $\Delta V$  values of both the PE and PC bilayer membranes were comparable while the  $\Delta H$  value was larger for the PE bilayer membrane. This suggests that the volume change at the  $L_c/L_\alpha$  transition of the

18:0-PE bilayer membrane is similar to that of the 18:0-PC bilayer membrane. Therefore, we can say that the volume of the  $L_c$  phase of PC series approaches that of PE series with an increase in chain length although the hydration states between both molecules are so different as described above.

#### 4.3. Thermodynamic properties for phase transitions of unsaturated diacyl-PE bilayer membranes

For the unsaturated PE bilayer membranes, the  $\Delta H$  and  $\Delta V$  values of the  $L_\alpha/H_{II}$  transition for the 18:1(*cis*)-PE and 18:1(*trans*)-PE bilayer membranes were extremely smaller than those of the  $L_c/L_\alpha$  transition for the 18:1(*cis*)-PE bilayer membrane and the  $L_\beta/L_\alpha$  transition for the 18:1(*trans*)-PE bilayer membrane, respectively, although the  $dT/dp$  values of the  $L_\alpha/H_{II}$  transition became larger than those of the  $L_c/L_\alpha$  and  $L_\beta/L_\alpha$  transitions. The  $L_\alpha/H_{II}$  transition corresponds to a packing change between bilayer and nonbilayer membranes. They produce a large transformation from a lamellar structure to an inverted hexagonal structure. However, in the  $L_\alpha/H_{II}$  transition, the order of hydrophobic chains of the PE molecules may not change appreciably at a phase below and above the transition, namely they take low-ordered chain conformation including *gauche* forms in both phases. Therefore, judging from the smaller thermodynamic quantities, we can say that the difference in thermodynamic state between both phases is small. Contrary to this, because the  $L_\beta/L_\alpha$  transition and  $L_c/L_\alpha$  transitions involve chain melting, and hence a large change in chain order, they also display a large change in entropy and volume. On the other hand, the  $dT/dp$  values were conversely larger in the  $L_\alpha/H_{II}$  transitions, which implies the transformation between  $L_\alpha$  and  $H_{II}$  structures is markedly influenced by pressure. A similar tendency was found in other bilayer-nonbilayer transitions such as interdigitation of dialkyl-PC bilayer membranes [15,19].

We next consider the thermal and volume contributions to each transition by comparing the  $\Delta H$  and  $\Delta V$  values of the bilayer-nonbilayer ( $L_\alpha/H_{II}$ ) transition with those of the bilayer-

bilayer ( $L_c/L_\alpha$  or  $L_\beta/L_\alpha$ ) transitions. The ratios of the  $\Delta H$  and  $\Delta V$  values between bilayer-nonbilayer and bilayer-bilayer transitions are listed in Table 3. The volume contribution was larger than the thermal contribution in  $L_\alpha/H_{II}$  transition, especially for the 18:1(*cis*)-PE bilayer membrane, the former contribution became more than twice larger than the latter contribution. It is further noticed that the bilayer membrane of 18:1(*cis*)-PE with *cis* double bonds exhibits the greater pressure-responsivity than that of 18:1(*trans*)-PE with *trans* double bonds, indicating that the formation of the  $H_{II}$  phase is markedly influenced by the geometrical difference in unsaturated acyl chains of a PE molecule. Taking into account that the large volume contribution of the  $L_\alpha/H_{II}$  transition reflects the large  $dT/dp$  value characteristic of the transition through the Clapeyron's equation, it turned out that the  $L_\alpha/H_{II}$  transition can be regarded as the transition dominated by volume contribution as comparison to enthalpic contribution, in other words, the volume-driven transition for the reconstruction of molecular packing.

#### *4.4. Comparison of thermodynamic properties between unsaturated diacyl-PE and diacyl-PC bilayer membranes*

Figure 7 compares the pressure dependence of temperatures of the transitions related to the  $L_\alpha$  phase ( $L_c/L_\alpha$  and  $gel/L_\alpha$  transitions) for the 18:0-PE, 18:1(*cis*)-PE and 18:1(*trans*)-PE bilayer membranes together with the corresponding results of bilayer membranes of PC series (18:0-PC, 18:1(*cis*)-PC and 18:1(*trans*)-PC) [18,21,50] to examine the effect of the introduction of double bonds into acyl chains on the phase transitions. Both PE and PC series showed almost similar phase-transition behavior: the transition temperature decreased in the order of bilayer membranes of saturated-form lipids, *trans*-form lipids and *cis*-form lipids, and the introduction effect of two *cis* double bonds to both chains is significantly larger than that of two *trans* double bonds. Since the thermodynamic quantities of the transitions related to the  $L_\alpha$  phase for the 18:1(*cis*)-PE and 18:1(*trans*)-PE bilayer membranes were also

comparable to those for the 18:1(*cis*)-PC and 18:1(*trans*)-PC bilayer membranes (cf. Table 2 for the PE series and tables in our previous studies [18,50] for the PC series), the resemblance of the thermodynamic quantities was also applicable to the case of the unsaturated lipids as well as the case of the saturated lipids given in Fig. 6. It should be noted that the  $dT/dp$  value and thermodynamic quantities of the  $L_c/L_\alpha$  transition for the 18:1(*cis*)-PE bilayer membrane had close values to those for the 18:1(*cis*)-PC bilayer membrane, supporting that the transition is the  $L_c/L_\alpha$  transition. However, the temperatures of the transition related to the  $L_\alpha$  phase for the PE series were higher than those for the PC series. We can also say that the strong attractive interaction between polar head groups of the unsaturated PE molecules in the bilayer membrane elevates the transition temperature as the case of the saturated PE bilayer membranes. Furthermore, the discussion of hydration difference between the saturated PE and PC bilayer membranes essentially may hold true for the unsaturated PE and PC bilayer membranes. The existence of the  $L_\beta$  phase in the DOPC bilayer membrane but not in the DOPE one is related to the difference in hydration of PC and PE head groups. In the DOPE bilayer membrane, the decrease in interlamellar water molecules at low temperature below the freezing point of water prevents the bilayer membrane from converting the  $L_\beta$  phase. Then, the  $L_c$  phase can only be observed in the DOPE bilayer membrane.

Here, comparing Fig. 7 with Fig. 3, we notice that the phase diagram of the 18:1(*cis*)-PC bilayer membrane qualitatively resembles those of the 16:0-PE and 18:0-PE bilayer membranes: their gel phases exist as the stable phase only under high pressure region in common. 16:0-PE or 18:0-PE with saturated acyl chains and a small sized head group is markedly different in molecular structure from 18:1(*cis*)-PC with unsaturated acyl chains and a large sized head group, and hence it is considered that the interaction between lipid molecules in the gel phase of the former PE bilayer membranes is much stronger than that of the latter PC bilayer membrane. Although there is a difference that the gel-phase stability of the 16:0-PE and 18:0-PE bilayer membranes changes in the region of high temperature and low pressure while that of the 18:1(*cis*)-PC one does in the region of low temperature and

high pressure, this resemblance in phase states between both lipids suggests that unsaturated lipids can take similar phase behavior to saturated lipids depending on temperature and pressure.

#### 4.5. Thermodynamic phase behavior of diacyl-PE bilayer membranes

Finally, it is useful to understand the change in phase behavior of the present PE bilayer membranes depending on temperature, pressure, chain length and chain unsaturation from the thermodynamic point of view. The fundamental phase states for lipid bilayer membranes are three: the  $L_c$ ,  $L_\beta$  and  $L_\alpha$  phases. Figure 8 illustrates the temperature dependence of free energies, namely isobaric curves of chemical potentials, at various pressures to consider the phase stability. In this figure, the slope of a curve corresponds to the entropy of each state. Pressure varies by the same intervals and the movement to the right side is the direction of pressurization. The temperature at which two chemical potential curves intersect is the phase-transition temperature. The  $L_\beta$  phase is metastable in the left side region in the figure (low temperature and low pressure) and the  $L_\beta/L_\alpha$ -transition temperature is lower than the  $L_c/L_\alpha$ -transition temperature. This behavior corresponds to the phase diagrams of the 12:0-PE and 14:0-PE bilayer membranes in the whole pressure range and the phase diagrams of the 16:0-PE and 18:0-PE bilayer membranes in the lower-pressure range. The increase of acyl chain length in the PE molecule makes the chemical-potential curve move into the right side region. The 18:1(*cis*)-PE bilayer membrane undergoes only the  $L_c/L_\alpha$  transition in the present study. This behavior is understandable that the phase stability of the 18:1(*cis*)-PE bilayer membrane corresponds to further left side region where the temperature difference between the  $L_c/L_\alpha$  and  $L_\beta/L_\alpha$  transitions becomes larger. In this region, the  $L_\beta$  phase is no longer metastable but unstable due to the great depression of the  $L_\beta/L_\alpha$ -transition temperature. On the other hand, three phases,  $L_c$ ,  $L_\beta$  and  $L_\alpha$  phases can be observed as all stable phases in the right side region in Fig. 8 (high temperature and high pressure). This behavior

corresponds to the phase diagrams of the 16:0-PE and 18:0-PE bilayer membranes in the high-pressure range. Usually, the detection of the  $L_c$  phase is required the suitable thermal annealing treatment of lipid samples such as long-term cold storage. Insufficient annealing treatment hinders the formation of the  $L_c$  phase, as a result, the  $L_\beta/L_\alpha$  transition instead of the  $L_c/L_\alpha$  transition as a metastable phase (broken-line region in Fig. 8) appears.

The chemical potential curve is closely related to the lipid molecular structure: the curves of PE bilayer membranes are generally located in the left side region while those of PC bilayer membranes are located in the right side region. The curve of long-chain saturated PC bilayer membranes become more complicated because the  $L_\beta$  phase separates into the  $L_\beta'$ ,  $P_\beta'$  and  $L_\beta I$  phases due to the gel-phase polymorphism. Pressurization makes the curve move to the right side region, whereas the substitution of unsaturated acyl chains for saturated chains conversely does the curve move to the left side region. Concerning the  $H_{II}$  phase, the chemical-potential curve can easily be extended as straight lines with a slightly larger slope than the  $L_\alpha$  phase in the right side region of the  $L_\alpha$  phase (see the inset in Fig. 8) although the phase is only observable for certain lipids. In the case of the 18:1(*trans*)-PE bilayer membranes, we could not observe the phase transition related to the  $L_c$  phase in this study. However, taking into account that it takes a long time to form the  $L_c$  phase for a bilayer of a long chain saturated PE or PC with chain length of 18 and the acyl chain with a *trans* double bond in the condensed phase takes a similar chain conformation to the saturated chain, it is expected that the gel phase may exist as a stable phase. Then the isobaric chemical potential curve of the 18:1(*trans*)-PE bilayer membranes may be located in the right side region like the long chain saturated PC bilayer membrane. Similarly, isothermal curves of chemical potentials can also be considered [18]. The phase behavior of various kinds of lipid bilayer membranes can be predicted by using these chemical potential curves.

## 5. Conclusions

Thermotropic and barotropic phase transitions of the saturated and unsaturated PE bilayer membranes were examined in this study. The  $T$ - $p$  phase diagrams and thermodynamic quantities of the phase transitions of the saturated and unsaturated PE bilayer membranes showed the characteristic behavior. The stability of the gel phase for the saturated PE bilayer membranes changed from metastable to stable depending on pressure and chain length, and there was no gel-phase polymorphism observed for the corresponding PC bilayer membranes. The  $L_c$  phase formed by the saturated PE molecules was more stable than that formed by PC molecules although the chain-melting behavior of both PE and PC bilayer membranes was almost comparable to each other. These findings are attributable to the strong interaction between small-sized polar head groups of the PE molecules with small numbers of interlamellar water molecules in the bilayer membrane. This stronger interaction also contributes to the higher phase-transition temperature of the PE bilayer membranes. On the other hand, the unsaturated PE bilayer membranes exhibited the greater reduction of phase-transition temperatures than the saturated PE ones like the case of the corresponding PC ones. The contrasting feature of the unsaturated PE bilayer membranes as compared with the PC ones is the formation of non-bilayer  $H_{II}$  phase at higher temperatures. The high-pressure responsiveness of the  $L_\alpha/H_{II}$  transition proved that the transition is the volume-driven transition for the reconstruction of molecular packing and simultaneously is subject to the geometrical structure of acyl chains of a lipid molecule. When considering the chemical potential curves depending on several influencing factors on the phase transitions, the phase transitions of lipid bilayer membranes can be comprehensively interpreted from the thermodynamic point of view.

## **Acknowledgments**

The authors wish to express their appreciation to the anonymous reviewers for their useful and valuable comments, which helped to upgrade the manuscript. This study was supported in part by a Grant-in Aid for Scientific Research (C) (2) (26410016) from Japan Society for the Promotion of Science.



## References

- [1] M. Caffrey, LIPIDAT, A Database of Thermodynamic Data and Associated Information on Lipid Mesomorphic and Polymorphic Transition, CRC Press, Boca Raton, Florida, 1993.
- [2] R. Koynova, M. Caffrey, Phases and phase transitions of the phosphatidylcholines, *Biochim. Biophys. Acta* 1376 (1998) 91-145.
- [3] D. Marsh, Handbook of Lipid Bilayers, 2nd ed., CRC Press, New York, 2013.
- [4] N. D. Russell, P. J. Collings, High pressure measurements in phospholipid bilayers using adiabatic compression, *J. Chem. Phys.* 77 (1982) 5766-5770.
- [5] P. L. G. Chong, G. Weber, Pressure dependence of 1,6-diphenyl-1,3,5-hexatrien fluorescence in single-component phosphatidylcholine liposomes, *Biochemistry* 22 (1983) 5544-5550.
- [6] S. Utoh, T. Takemura, Phase transition of lipid multilamellar aqueous suspension under high pressure: I. Investigation of phase diagram of dipalmitoylphosphatidylcholine bimembrane by high pressure-DTA and -dilatometry, *Jpn. J. Appl. Phys.* 24 (1985) 356-360.
- [7] P. T. T. Wong, H. H. Mantsch, Effects of hydrostatic pressure on the molecular structure and endothermic phase transitions of phosphatidylcholine bilayers: A Raman scattering study, *Biochemistry* 24 (1985) 4091-4096.
- [8] L. F. Braganza, D. L. Worcester, Hydrostatic pressure induces hydrocarbon chain interdigitation in single-component phospholipid bilayers, *Biochemistry* 25 (1986) 2591-2596.
- [9] S. K. Prasad, R. Shashidhar, B. P. Gaber, S. C. Chandrasekhar, Pressure studies on two hydrated phospholipids – 1,2-dimristoyl-phosphatidylcholine and 1,2-dipalmitoyl-phosphatidylcholine, *Chem. Phys. Lipids* 43 (1987) 227-235.

- [10] R. Winter, W. C. Pilgrim, A SANS study of high pressure phase transitions in model biomembranes, *Ber. Bunsenges. Phys. Chem.* 93 (1989) 708-717.
- [11] D. A. Driscoll, J. Samarasinghe, S. Adamy, J. Jonas, A. Jonas, Pressure effects on dipalmitoylphosphatidylcholine bilayers measured by  $^2\text{H}$  nuclear magnetic resonance, *Biochemistry* 30 (1991) 3322-3327.
- [12] S. A. Potekhin, A. A. Senin, N. N. Abdurakhmanov, R. S. Khusainova, High pressure effect on the main transition from the ripple gel ( $P_{\beta}'$ ) phase to the liquid crystal ( $L_{\alpha}$ ) phase in dipalmitoylphosphatidylcholine. Microcalorimetric study, *Biochim. Biophys. Acta* 1778 (2008) 2588-2593.
- [13] S. A. Potekhin, A. A. Senin, N. N. Abdurakhmanov, R. S. Khusainova, Thermodynamic invariants of gel to the liquid-crystal 1,2-diacylphosphatidylcholines transition, *Biochim. Biophys. Acta* 1808 (2011) 1806-1810.
- [14] S. A. Potekhin, A. A. Senin, R. S. Khusainova, Thermodynamics of the gel to liquid crystal 1,2-diacylphosphatidylcholines transition. High-pressure microcalorimetry, *Thermochim. Acta* 560 (2013) 17-26.
- [15] S. Maruyama, H. Matsuki, S. Kaneshina, Thermotropic and barotropic phase behavior of dihexadecylphosphatidylcholine bilayer membrane, *Chem. Phys. Lipids* 82 (1996) 125-132.
- [16] H. Ichimori, T. Hata, T. Yoshioka, H. Matsuki, S. Kaneshina, Thermotropic and barotropic phase transition on bilayer membranes of phospholipids with varying acyl chain-lengths, *Chem. Phys. Lipids* 89 (1997) 97-105.
- [17] H. Ichimori, T. Hata, H. Matsuki, S. Kaneshina, Barotropic phase transitions and pressure-induced interdigitation on bilayer membranes of phospholipids with varying acyl chain-lengths, *Biochim. Biophys. Acta* 1414 (1998) 165-174.
- [18] H. Ichimori, T. Hata, H. Matsuki, S. Kaneshina, Effect of unsaturated acyl chains on the thermotropic and barotropic phase transitions of phospholipid bilayer membranes, *Chem. Phys. Lipids* 100 (1999) 151-154.

- [19] H. Matsuki, E. Miyazaki, F. Sakano, N. Tamai, S. Kaneshina, Thermotropic and barotropic phase transitions in bilayer membranes of ether-linked phospholipids with varying alkyl chain lengths, *Biochim. Biophys. Acta* 1768 (2007) 479-489.
- [20] M. Goto, S. Ishida, N. Tamai, H. Matsuki, S. Kaneshina, Chain asymmetry alters thermotropic and barotropic properties of phospholipid bilayer membranes, *Chem. Phys. Lipids* 161 (2009) 65-76.
- [21] H. Matsuki, M. Goto, K. Tada, N. Tamai, Thermotropic and barotropic phase behavior of phosphatidylcholine bilayers, *Int. J. Mol. Sci.* 14 (2013) 2282-2302.
- [22] M. Goto, T. Endo, T. Yano, N. Tamai, J. Kohlbrecher, H. Matsuki, Comprehensive characterization of temperature- and pressure-induced phase transitions for saturated phosphatidylcholines containing longer chain homologs, *Colloids Surf. B: Biointerf.* 128 (2015) 389-397.
- [23] D. J. Vaughan, K. M. Keough, Changes in phase transitions of phosphatidylethanolamine- and phosphatidylcholines-water dispersions induced by small modifications in the headgroup and backbone regions, *FEBS Lett.* 47 (1974) 158-161.
- [24] P. R. Cullis, B. De Kruijff, The polymorphic phase behaviour of phosphatidylethanolamines of natural and synthetic origin, *Biochim. Biophys. Acta* 513 (1978) 31-42.
- [25] D. A. Wilkinson, J. F. Nagle, Dilatometry and calorimetry of phosphatidylethanolamine dispersions, *Biochemistry* 20 (1981) 187-192.
- [26] H. H. Mantsch, S. C. His, K. W. Butler, D. G. Cameron, Studies on the thermotropic behavior of aqueous phosphatidylethanolamines, *Biochim. Biophys. Acta* 728 (1983) 325-330.
- [27] J. M. Seddon, K. Harlos, D. Marsh, Metastability and polymorphism in the gel and fluid bilayer phases of dilauroylphosphatidylethanolamine, *J. Biol. Chem.* 258 (1983) 3850-3854.

- [28] D. A. Wilkinson, J. F. Nagle, Metastability in the phase behavior of dimyristoylphosphatidylethanolamine bilayers, *Biochemistry* 23 (1984) 1538-1541.
- [29] J. R. Silvius, P. M. Brown, T. J. O'Leary, Role of head group structure in the phase behavior of amino phospholipids. 1. Hydrated and dehydrated lamellar phases of saturated phosphatidylethanolamine analogues, *Biochemistry* 25 (1986) 4249-4258.
- [30] H.-D. Dörfler, G. Brezesinski, P. Miethe, Phase diagrams of pseudo-binary phospholipid systems I. Influence of the chain length differences on the miscibility properties of cephaline/cephaline/water systems, *Chem. Phys. Lipids* 48 (1988) 245-254.
- [31] R. Koynova, H.-J. Hinz, Metastable behaviour of saturated phosphatidylethanolamines: a densitometric study, *Chem. Phys. Lipids* 54 (1990) 67-72.
- [32] M. A. Singer, L. Finegold, P. Rochon, T. J. Racey, The formation of multilamellar vesicles from saturated phosphatidylcholines and phosphatidylethanolamines: morphology and quasi-elastic light scattering measurements, *Chem. Phys. Lipids* 54 (1990) 131-146.
- [33] R. N. A. H. Lewis, R. N. McElhaney, Calorimetric and spectroscopic studies of the polymorphic phase behavior of a homologous series of *n*-saturated 1,2-diacyl phosphatidylethanolamines, *Biophys. J.* 64 (1993) 1081-1096.
- [34] R. Koynova, M. Caffrey, Phases and phase transitions of the hydrated phosphatidylethanolamines, *Chem. Phys. Lipids* 69 (1994) 1-34.
- [35] R. M. Epand, High sensitivity differential scanning calorimetry of the bilayer to hexagonal phase transitions of diacylphosphatidylethanolamines, *Chem. Phys. Lipids* 36 (1985) 387-393.
- [36] P. M. Brown, J. Steers, S. W. Hui, P. L. Yeagle, J. R. Silvius, Role of head group structure in the phase behavior of amino phospholipids. 2. Lamellar and nonlamellar phases of unsaturated phosphatidylethanolamine analogues, *Biochemistry* 25 (1986) 4259-4267.

- [37] R. M. Epand, R. F. Epand, Kinetic effects in the differential scanning calorimetry cooling scans of phosphatidylethanoamines, *Chem. Phys. Lipids* 49 (1988) 101-104.
- [38] K. Gawrisch, V. A. Parsegian, D. A. Hajduk, M. W. Tate, S. M. Gruner, N. L. Fuller, R. P. Rand, Energetics of a hexagonal-lamellar-hexagonal phase transition sequence in dioleoylphosphatidylethanolamine membranes, *Biochemistry* 31 (1992) 2856-2864.
- [39] R. N. A. H. Lewis, D. A. Mannock, R. N. McElhaney, Effect of fatty acyl chain length and structure on the lamellar gel to liquid-crystalline and lamellar to reversed hexagonal phase transitions of aqueous phosphatidylethanolamine dispersions, *Biochemistry* 28 (1989) 541-548.
- [40] D. Marsh, Analysis of the chainlength dependence of lipid phase transition temperatures: Main and pretransitions of phosphatidylcholines; main and non-lamellar transitions of phosphatidylethanolamines, *Biochim. Biophys. Acta*, 1062 (1991) 1-6.
- [41] D. P. Siegel, R. M. Epand, The mechanism of lamellar-to-inverted hexagonal phase transitions in phosphatidylethanolamine: implications for membrane fusion mechanisms, *Biophys. J.* 73 (1997) 3089-3111.
- [42] E. Y. Shalaev, P. L. Steponkus, Phase diagram of 1,2-dioleoylphosphatidylethanolamine (DOPE): water system at subzero temperatures and at low water contents, *Biochim. Biophys. Acta*, 1419 (1999) 229-247.
- [43] P. E. Harper, D. A. Mannock, R. N. A. H. Lewis, R. N. McElhaney, S. M. Gruner, X-ray diffraction structures of some phosphatidylethanolamine lamellar and inverted hexagonal phases, *Biophys. J.* 81 (2001) 2693-2706.
- [44] G. E. S. Toombes, A. C. Finnefrock, M. W. Tate, S. M. Gruner, Determination of  $L_{\alpha}$  –  $H_{II}$  phase transition temperature for 1,2-dioleoyl-*sn*-glycero-3-phosphatidylethanolamine, *Biophys. J.* 82 (2002) 2504-2510.
- [45] S. M. Gruner, Nonlamellar lipid phases, in: P. L. Yeagle (Ed.), *The Structure of Biological Membranes*, 2nd ed., CRC Press, New York, 2005, pp. 173-199.

- [46] R. Sueyoshi, K. Tada, M. Goto, N. Tamai, H. Matsuki, S. Kaneshina, Barotropic phase transition between the lamellar liquid crystal phase and the inverted hexagonal phase of dioleoylphosphatidylethanolamine, *Colloids Surf. B: Biointerf.* 50 (2006) 85-88.
- [47] B. de Kruijff, Lipid polymorphism and biomembrane function, *Curr. Opin. Chem. Biol.* 1 (1997) 564-569.
- [48] W. Stillwell, *An Introduction to Biological Membranes*, Academic Press, San Diego, 2013, pp. 185-186.
- [49] L. K. Buehler, *Cell Membranes*, Garland Science, Taylor & Francis Group, LLC, New York, 2016, pp. 141-192.
- [50] M. Kusube, M. Goto, N. Tamai, H. Matsuki, S. Kaneshina, Bilayer phase transitions of *N*-methylated dioleoylphosphatidylethanolamines under high pressure, *Chem. Phys. Lipids* 142 (2006) 94-102.
- [51] M. Kusube, H. Matsuki, S. Kaneshina, Thermotropic and barotropic phase transitions of *N*-methylated dipalmitoylphosphatidylethanolamine bilayers, *Biochim. Biophys. Acta* 1668 (2005) 25-32.
- [52] R. Winter, J. Erbes, C. Czeslik, A. Gabke, Effect of pressure on the stability, phase behaviour and transformation kinetics between structures of lyotropic lipid mesophases and model membrane systems, *J. Phys.: Condens. Matter* 10 (1998) 11499-11518.
- [53] R. N. A. H. Lewis, N. Mak, R. N. McElhaney, A differential scanning calorimetric study of the thermotropic phase behavior of model membranes composed of phosphatidylcholines containing linear saturated fatty acyl chains, *Biochemistry* 26 (1987) 6118-6126.
- [54] R. N. A. H. Lewis, R. N. McElhaney, Subgel phases of *n*-saturated diacylphosphatidylcholines: a fourier-transform infrared spectroscopic study, *Biochemistry* 29 (1990) 7946-7953.

- [55] M. Kodama, H. Inoue, Y. Tsuchida, The behavior of water molecules associated with structural changes in phosphatidylethanolamine assembly as studied by DSC, *Thermochim. Acta* 266 (1995) 373-384.
- [56] H. Takahashi, H. Aoki, M. Kodama, I. Hatta, On exothermic transformation from metastable gel phase to stable crystalline phase of fully hydrated dimyristoylphosphatidylethanolamine in heating scan, *Chem. Phys. Lipids* 87 (1997) 83-89.
- [57] S. M. Gruner, M. W. Tate, G. L. Kirk, P. T. C. So, D. C. Turner, D. T. Keane, C. P. S. Tilcock, P. R. Cullis, X-ray diffraction study of the polymorphic behavior of *N*-methylated dioleoylphosphatidylethanolamine, *Biochemistry* 27 (1988) 2853-2866.
- [58] S. Kaneshina, H. Ichimori, T. Hata, H. Matsuki, Barotropic phase transitions of dioleoylphosphatidylcholine and stearyl-oleoylphosphatidylcholine bilayer membranes, *Biochim. Biophys. Acta* 1374 (1998) 1-8.
- [59] H. Matsuki, H. Okuno, F. Sakano, M. Kusube, S. Kaneshina, Effect of deuterium oxide on the thermodynamic quantities associated with phase transitions of phosphatidylcholine bilayer membranes, *Biochim. Biophys. Acta* 1712 (2005) 92-100.
- [60] K. Tada, M. Goto, N. Tamai, H. Matsuki, S. Kaneshina, Thermotropic and barotropic phase transitions of dilauroylphosphatidylcholine Bilayer, *Chem. Phys. Lipids* 153 (2008) 138-143.
- [61] T. J. McIntosh, S. A. Simon, Area per molecule and distribution of water in fully hydrated dilauroylphosphatidylethanolamine bilayers, *Biochemistry* 25 (1986) 4948-4952.
- [62] J. M. Boggs, Lipid intermolecular hydrogen bonding: influence on structural organization and membrane function, *Biochim. Biophys. Acta* 906 (1987) 353-404.
- [63] M. Kodama, T. Miyata, Effect of the head group of phospholipids on the acyl-chain packing and structure of their assemblies as revealed by microcalorimetry and electron microscopy, *Colloids Surf. A: Physicochem. Eng. Aspects* 109 (1996) 283-289.

- [64] H. Hauser, I. Pascher, R. H. Pearson, S. Sundell, Preferred conformation and molecular packing of phosphatidylethanolamine and phosphatidylcholine, *Biochim. Biophys. Acta* 650 (1981) 21-51.
- [65] S. Mulukutla, G. G. Shipley, Structure and thermotropic properties of phosphatidylethanolamine and its *N*-methyl derivatives, *Biochemistry* 23 (1984) 2514-2519.
- [66] I. Pascher, S. Sundell, Membrane lipids: preferred conformational states and their interplay. The crystal structure of dilauroyl-*N,N*-dimethylphosphatidylethanolamine, *Biochim. Biophys. Acta* 855 (1986) 68-78.
- [67] M. Kodama, H. Aoki, H. Takahashi, I. Hatta, Interlamellar waters in dimyristoylphosphatidylethanolamine-water system as studied by calorimetry and X-ray diffraction, *Biochim. Biophys. Acta* 1329 (1997) 61-73.
- [68] H. Aoki, M. Kodama, Calorimetric investigation of the behavior of interlamellar water in phospholipid-water systems, *Thermochim. Acta* 308 (1998) 77-83.
- [69] M. Kodama, H. Kato, H. Aoki, The behavior of water molecules in the most stable subgel phase of dimyristoylphosphatidylethanolamine-water system as studied by differential scanning calorimetry, *Thermochim. Acta* 352-353 (2000) 213-221.
- [70] M. Kodama, H. Kato, H. Aoki, Comparison of differently bound molecules in the gel and subgel phases of a phospholipid bilayer system, *J. Therm. Anal. Cal.* 64 (2001) 219-230.



## Figure Legends

Fig. 1. DSC heating thermograms of saturated and unsaturated PE bilayer membranes: (1) 12:0-PE, (2) 14:0-PE, (3) 16:0-PE, (4) 18:0-PE, (5) 18:1(*cis*)-PE, (6) 18:1(*trans*)-PE. A large ice-melting peak in the vicinity of 0°C was omitted in the figure.

Fig. 2. Typical curves for isobaric thermotropic phase transitions of saturated and unsaturated PE bilayer membranes: (a) 14:0-PE, (b) 18:0-PE, (c) 18:1(*trans*)-PE. Pressure: (a) (1) 1st scan at 0.1 MPa, (2) 2nd scan at 0.1 MPa, (3) 1st scan at 102 MPa, (4) 2nd scan at 102 MPa; (b) (1) 1st scan at 0.1 MPa, (2) 2nd scan at 0.1 MPa, (3) 1st scan at 47 MPa, (4) 2nd scan at 47 MPa; (c) (1) 0.1 MPa, (2) 62 MPa.

Fig. 3. Temperature-pressure phase diagrams of saturated PE bilayer membranes: (a) 12:0-PE, (b) 14:0-PE, (c) 16:0-PE, (d) 18:0-PE. Phase transitions: (□)  $L_c/L_\alpha$  or  $L_c/L_\beta$  transition, (○)  $L_\beta/L_\alpha$  transition. Solid and broken lines indicate the phase transition between stable phases and that between metastable phases, respectively.

Fig. 4. Temperature-pressure phase diagrams of unsaturated PE bilayer membranes: (a) 18:1(*cis*)-PE, (b) 18:1(*trans*)-PE. Phase transitions: (□)  $L_c/L_\alpha$  transition, (○)  $L_\beta/L_\alpha$  transition, (▽)  $L_\alpha/H_{II}$  transition.

Fig. 5. Effect of hydrophobic chain length on phase-transition temperatures of saturated phospholipid bilayer membranes: (□)  $L_c/L_\alpha$  transition, (○)  $L_\beta/L_\alpha$  transition, (■)  $L_c/gel$  transition, (●)  $P_\beta'/L_\alpha$  transition, (◆)  $L_c/L_x$  transition. Open and closed symbols correspond to values of saturated PE and PC bilayer membranes, respectively. For the bilayer membranes of saturated PCs except for 12:0-PC, the  $L_c/gel$  transitions are the  $L_c/P_\beta'$  transition for the 14:0-PC bilayer membrane and the  $L_c/L_\beta'$  transitions for the 16:0-PC and 18:0-PC bilayer membranes. For the 12:0-PC bilayer membrane, the temperature of the  $L_c/L_x$

transitions in the 50% ethylene glycol solution was plotted in the figure. The standard error bars are omitted because they are smaller than the size of the symbols.

Fig. 6. Effect of hydrophobic chain length on phase-transition (a) enthalpies and (b) volumes of saturated phospholipid bilayer membranes: ( $\square$ ,  $\blacksquare$ )  $L_c/L_\alpha$  transition, ( $\circ$ ,  $\bullet$ )  $gel/L_\alpha$  transition. Open and closed symbols correspond to values of saturated PE and saturated PC bilayer membranes, respectively. For the bilayer membranes of saturated PCs except for 12:0-PC, the values of the  $P_\beta'/L_\alpha$  transition and the cumulative values of the sub ( $L_c/L_\beta'$  or  $L_c/P_\beta'$ ), pre ( $L_\beta'/P_\beta'$ ) and main ( $P_\beta'/L_\alpha$ ) transition were used as those of the  $gel/L_\alpha$  transition and the  $L_c/L_\alpha$  transition, respectively. For the 12:0-PC bilayer membrane, the cumulative values of the  $L_c/L_x$  and  $L_x/L_\alpha$  transitions in the 50% ethylene glycol solution were used as those of the  $L_c/L_\alpha$  transition. The standard error bars are omitted because they are smaller than the size of the symbols.

Fig. 7. Comparison of the pressure dependence of temperatures of the transition related to the  $L_\alpha$  phase for saturated phospholipid bilayer membranes with those of unsaturated phospholipid bilayer membranes: (a) PE series; (1) 18:0-PE, (2) 18:1(*trans*)-PE, (3) 18:1(*cis*)-PE, (b) PC series; (1) 18:0-PC, (2) 18:1(*trans*)-PC, (3) and (4) 18:1(*cis*)-PC. The transition of the 18:1(*cis*)-PE bilayer membrane and those of other phospholipid bilayer membranes are the  $L_c/L_\alpha$  transition and the  $gel/L_\alpha$  ( $L_\beta/L_\alpha$  or  $P_\beta'/L_\alpha$  (18:0-PC)) transitions, respectively. The  $L_c/L_\alpha$  transition of 18:1(*cis*)-PC bilayer membrane is shown as the curve 4 in the figure (b) for comparison.

Fig. 8. Schematic diagram of chemical potential–temperature curves for the  $L_c$ ,  $L_\beta$  and  $L_\alpha$  phases. Solid and broken lines refer to stable and metastable states, respectively. The slopes reflect the partial molar entropies of phospholipids in each state. Break points on the chemical potential curves correspond to phase transition points. Isobaric curves are drawn at regular pressure intervals. The chemical potential–temperature curve for the  $H_{II}$  phase is drawn in the inset.

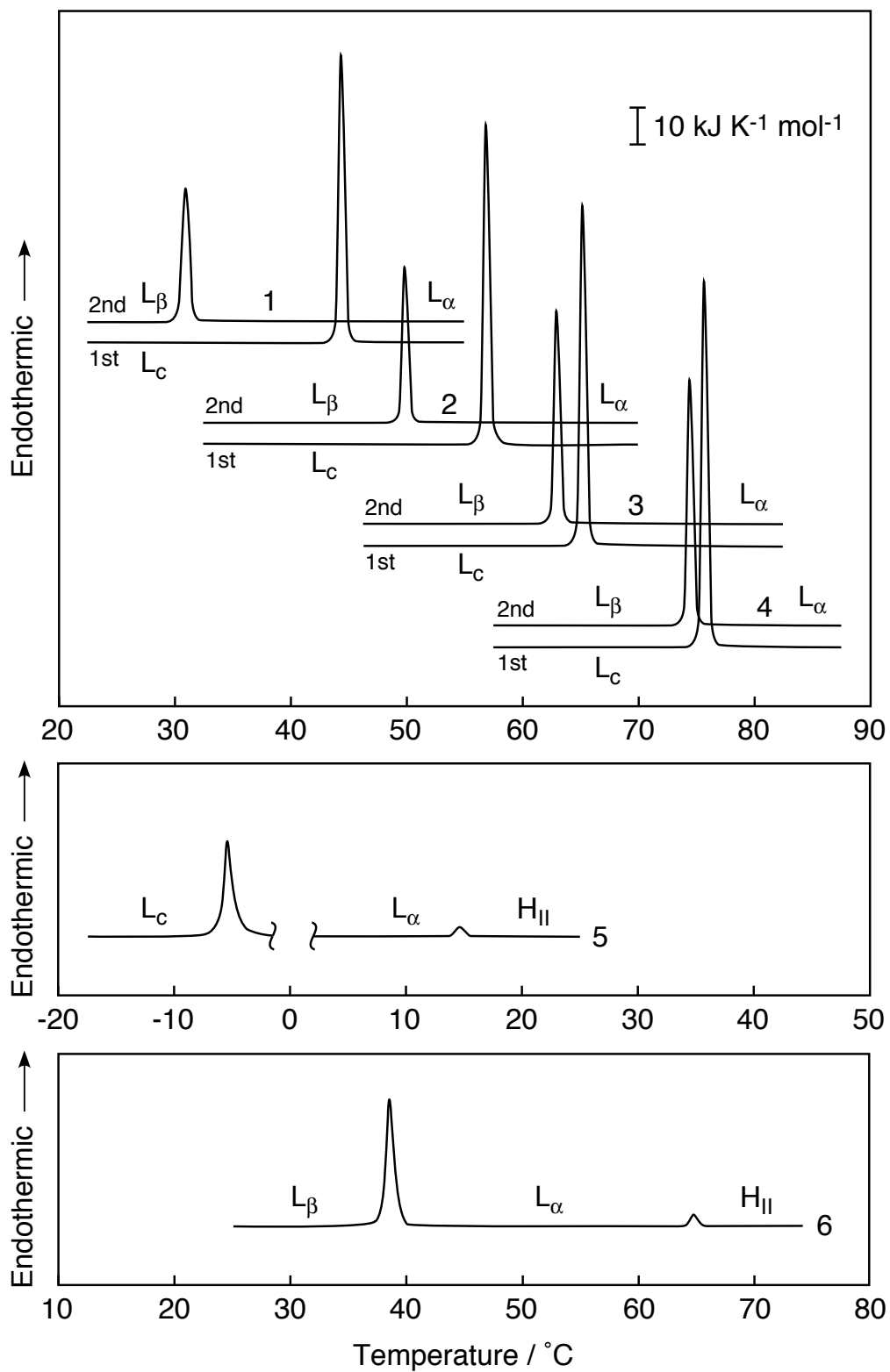


Fig. 1. Matsuki, et al.

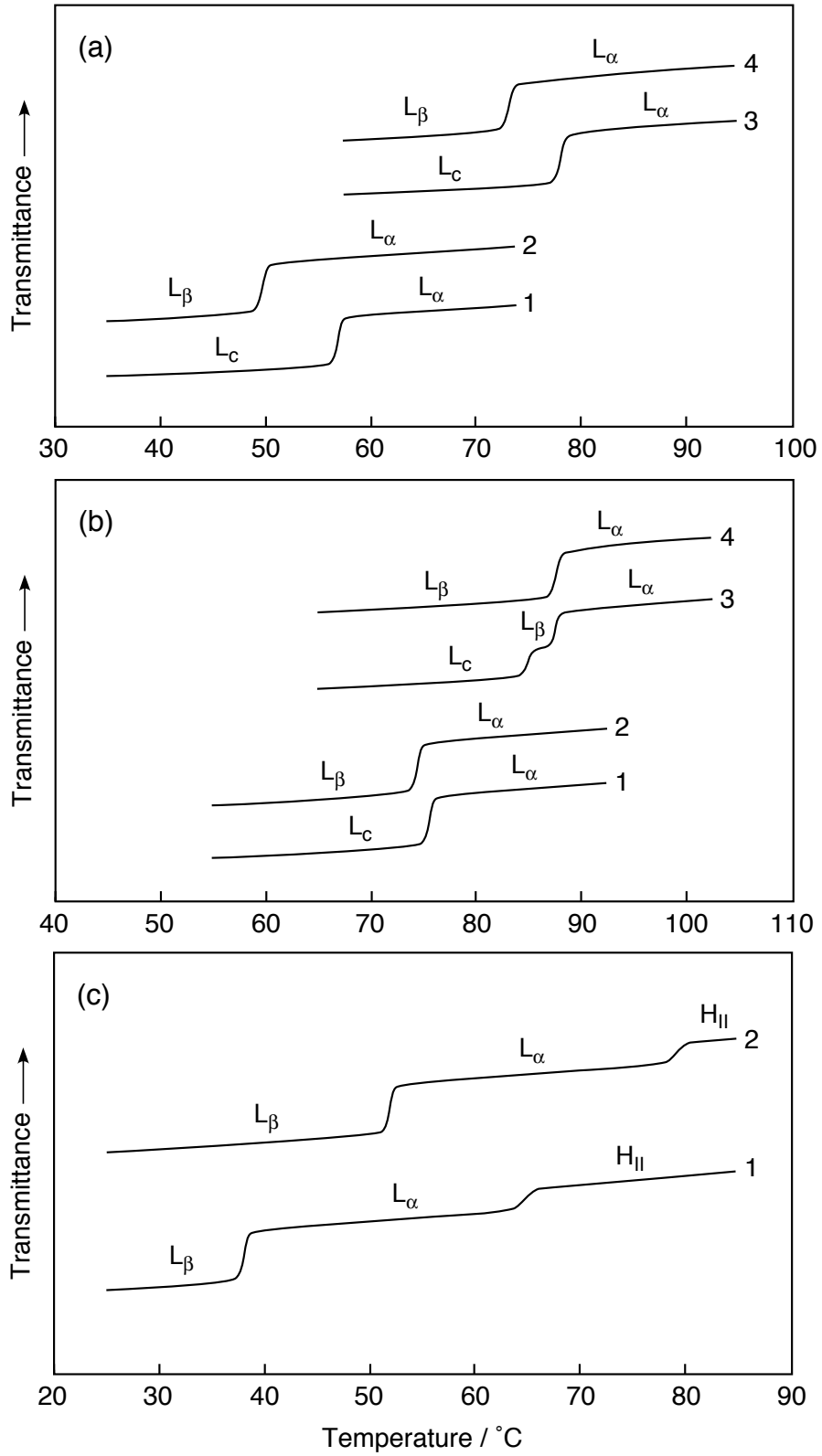


Fig. 2. Matsuki, et al.

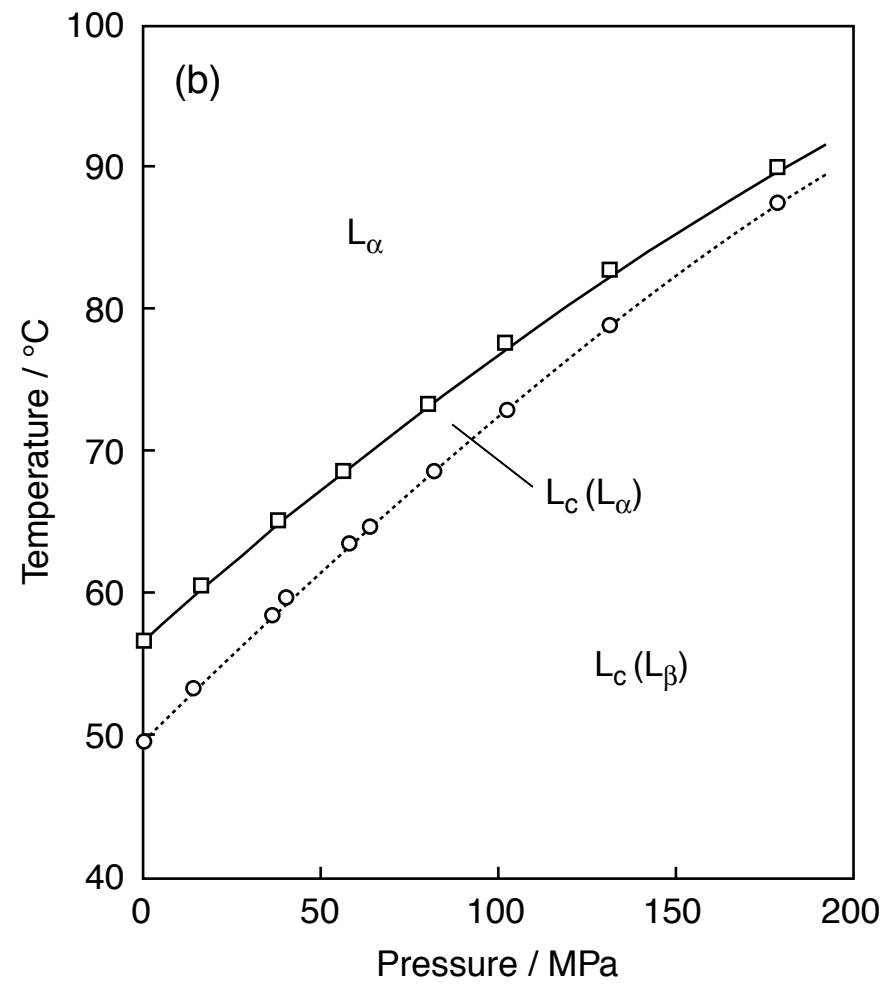
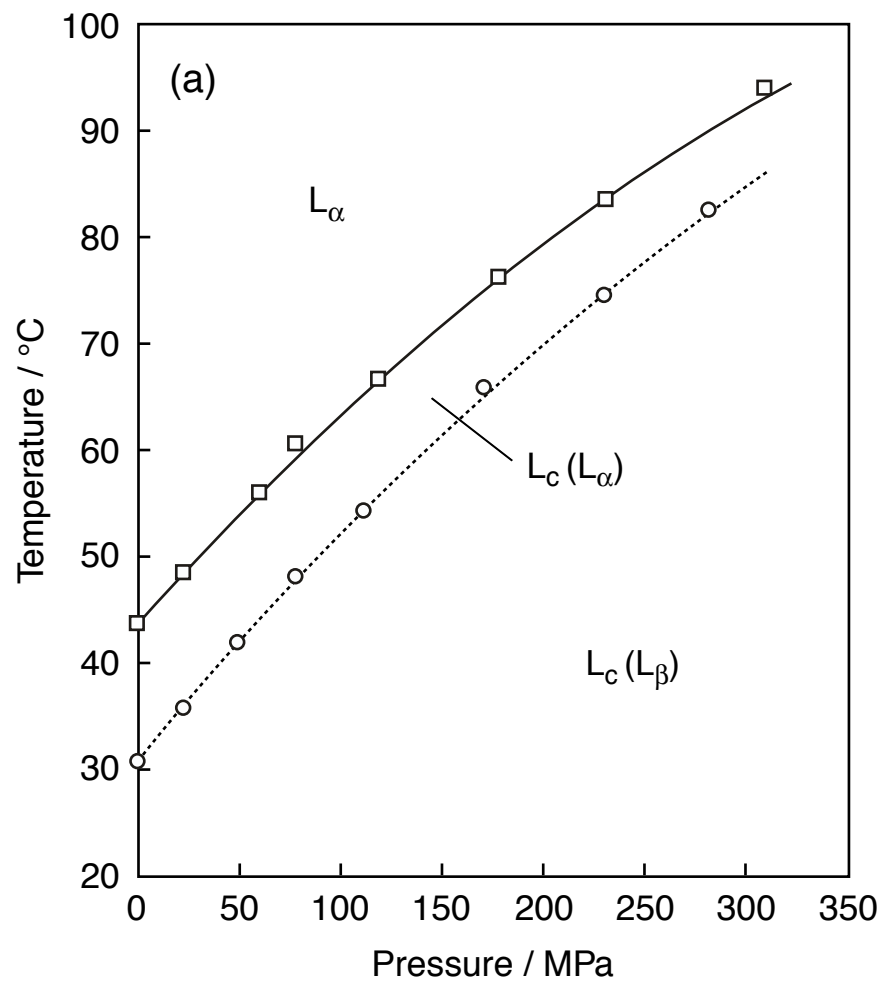


Fig. 3(1). Matsuki, et al.

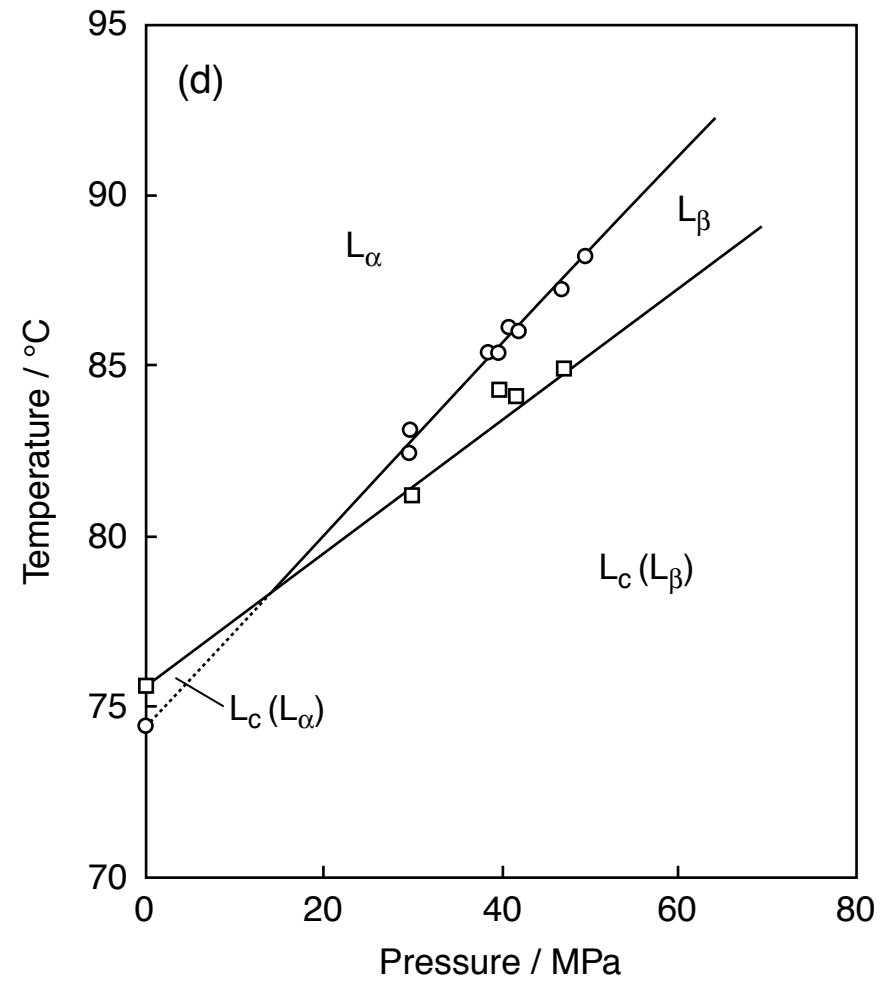
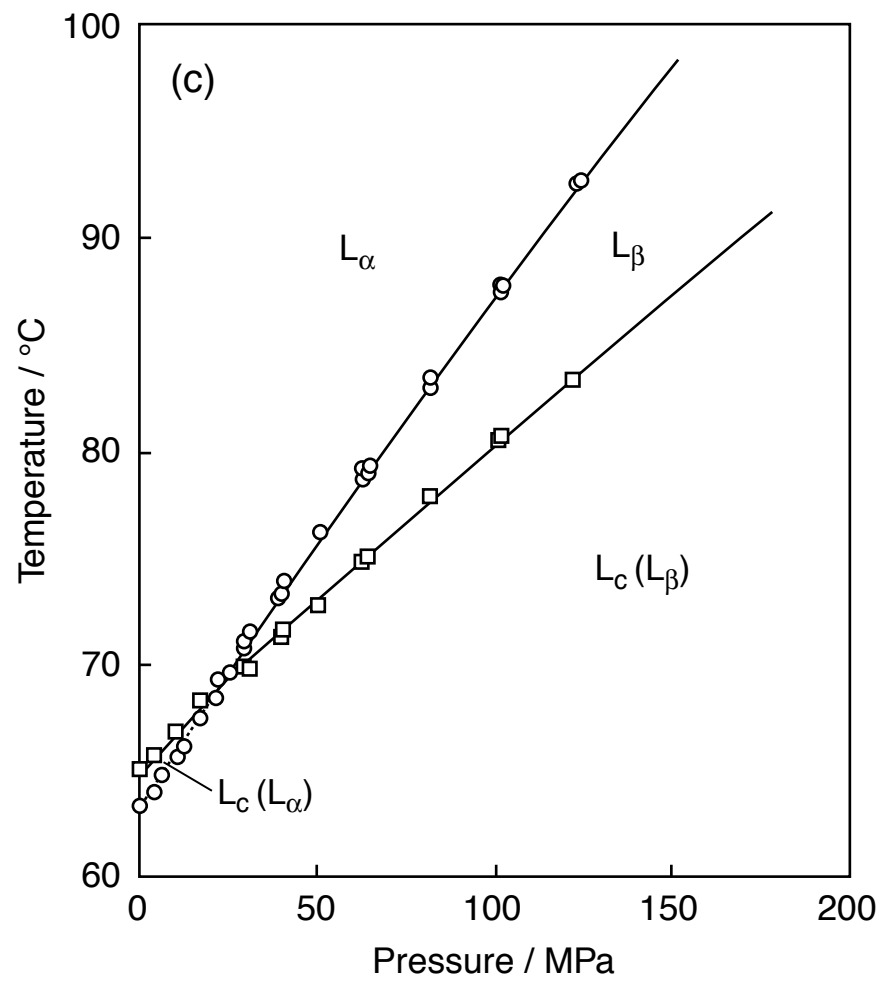


Fig. 3(2). Matsuki, et al.

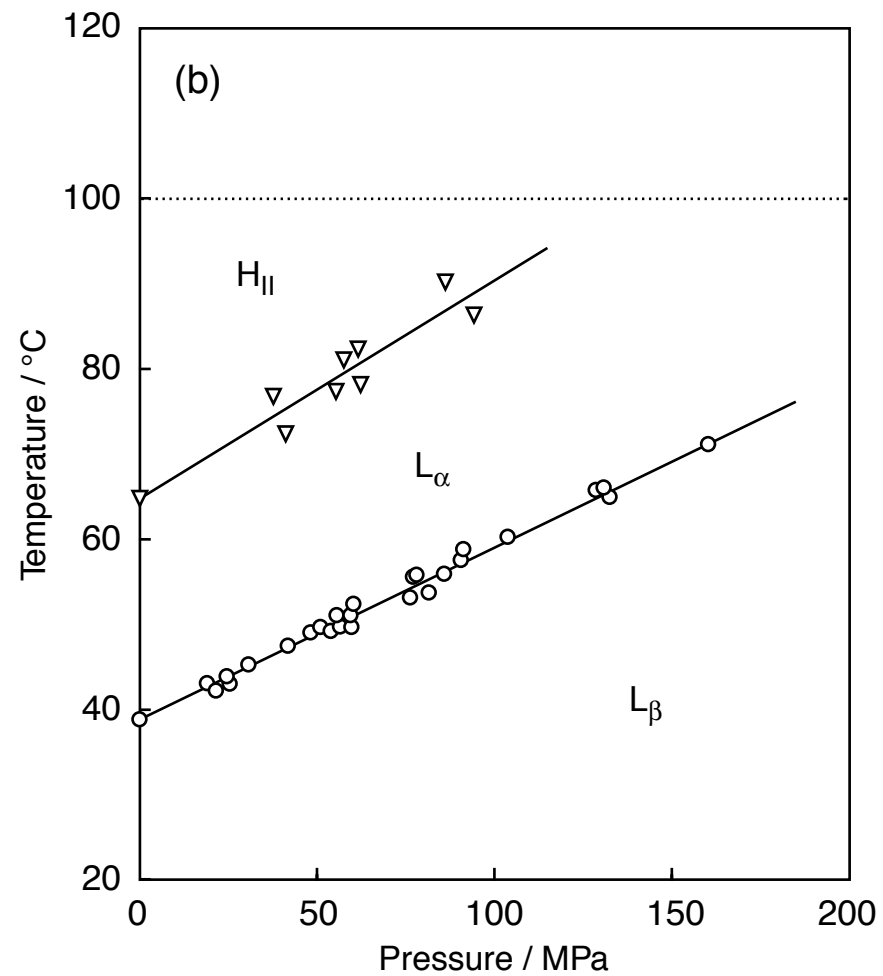
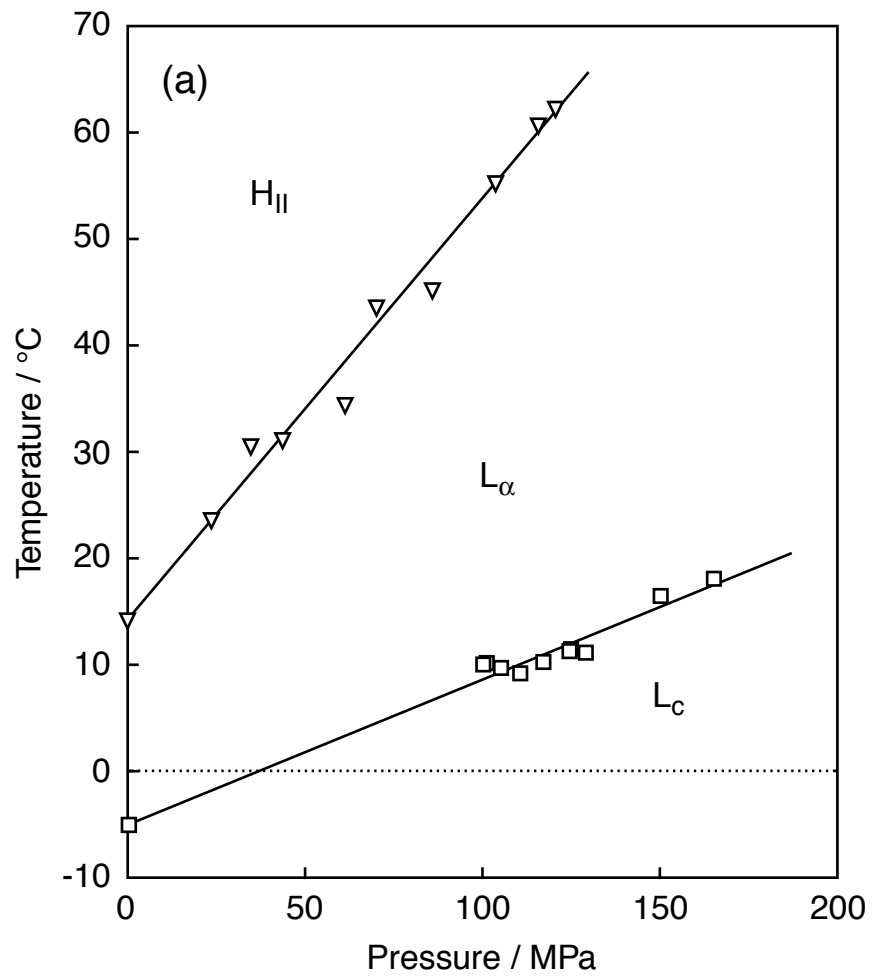


Fig. 4. Matsuki, et al.

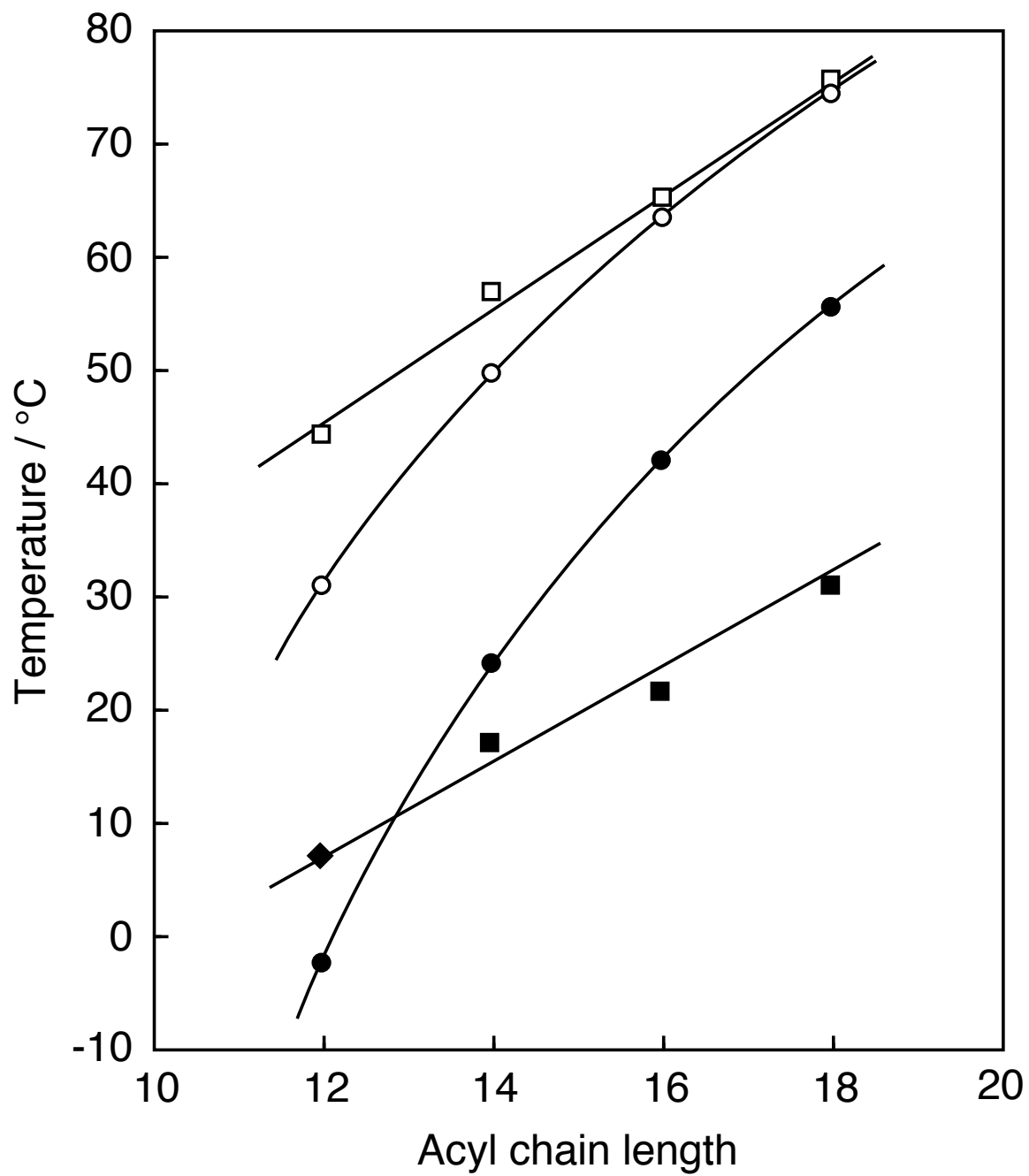


Fig. 5. Matsuki, et al.



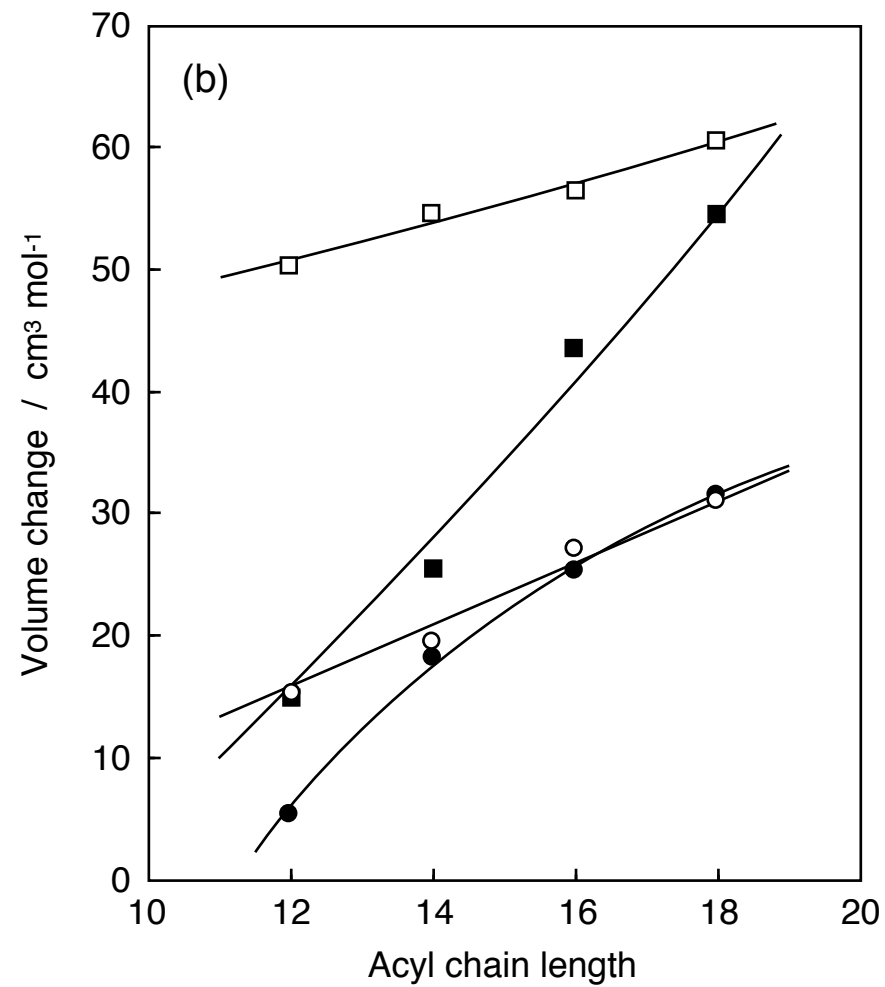
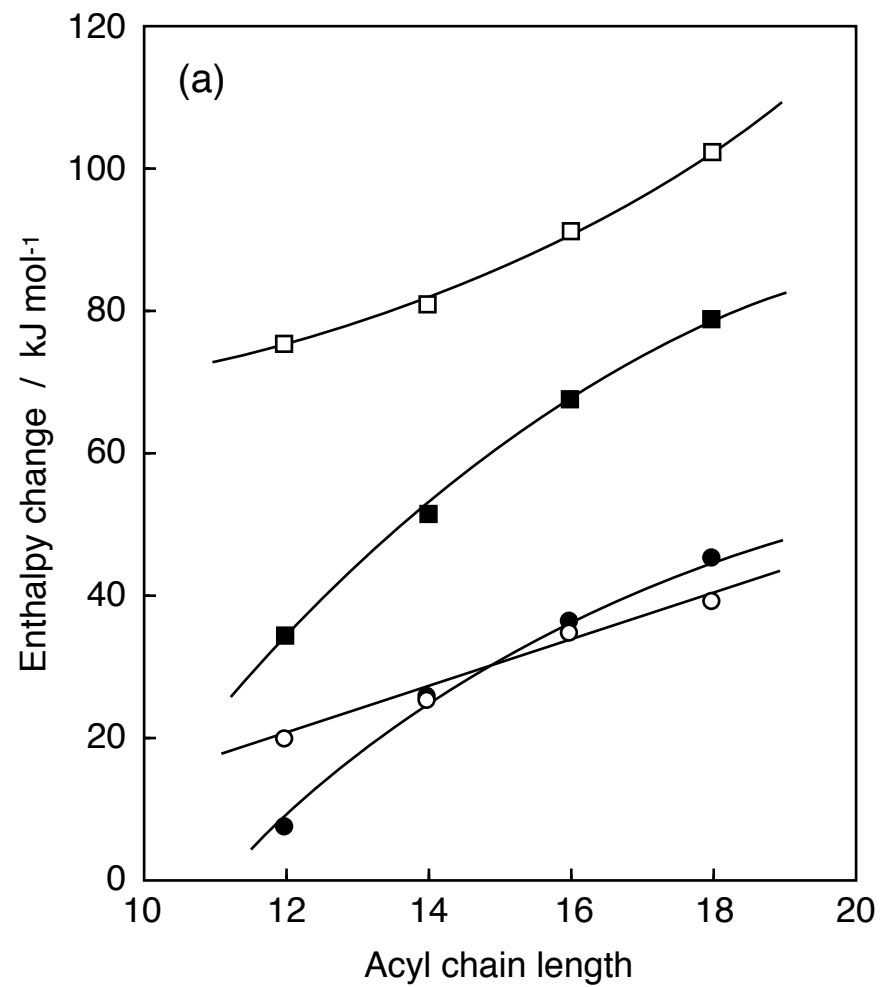


Fig. 6. Matsuki, et al.

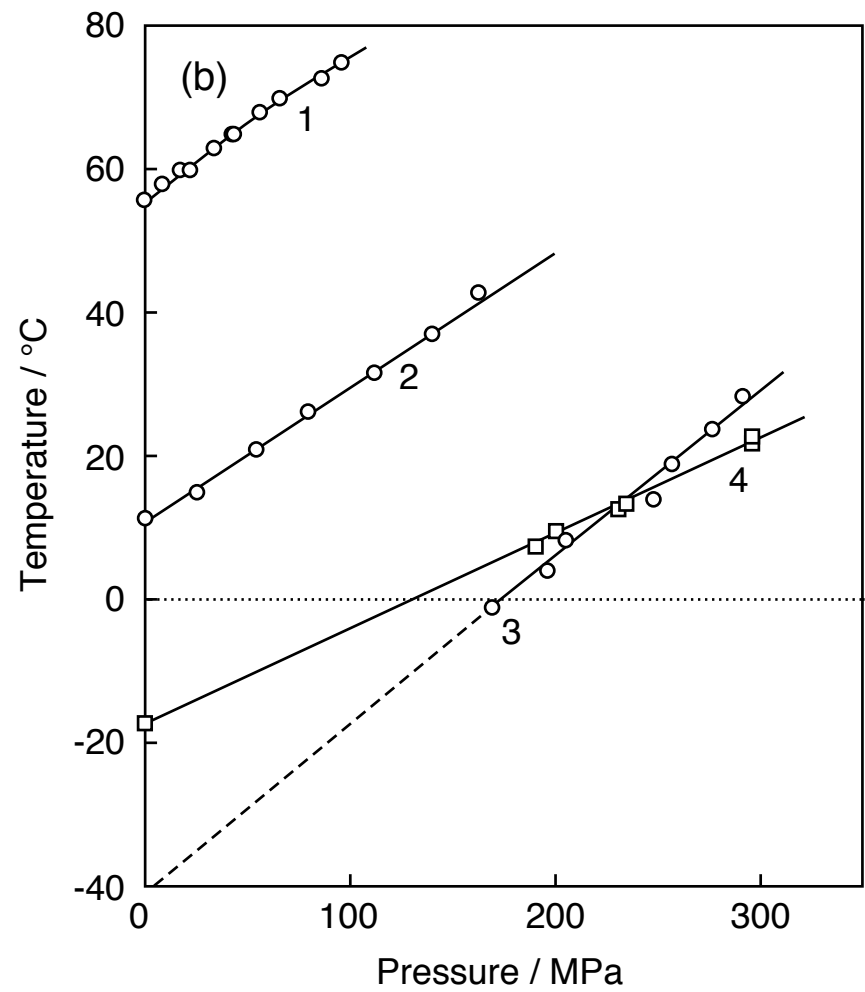
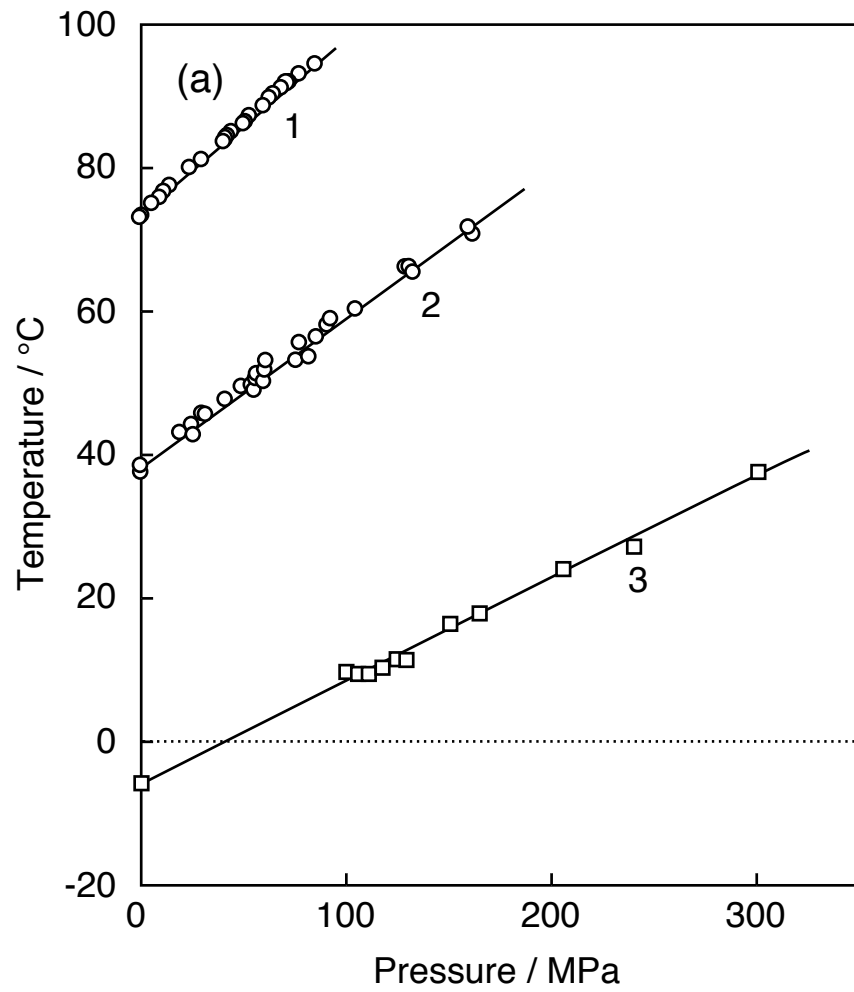


Fig. 7. Matsuki, et al.

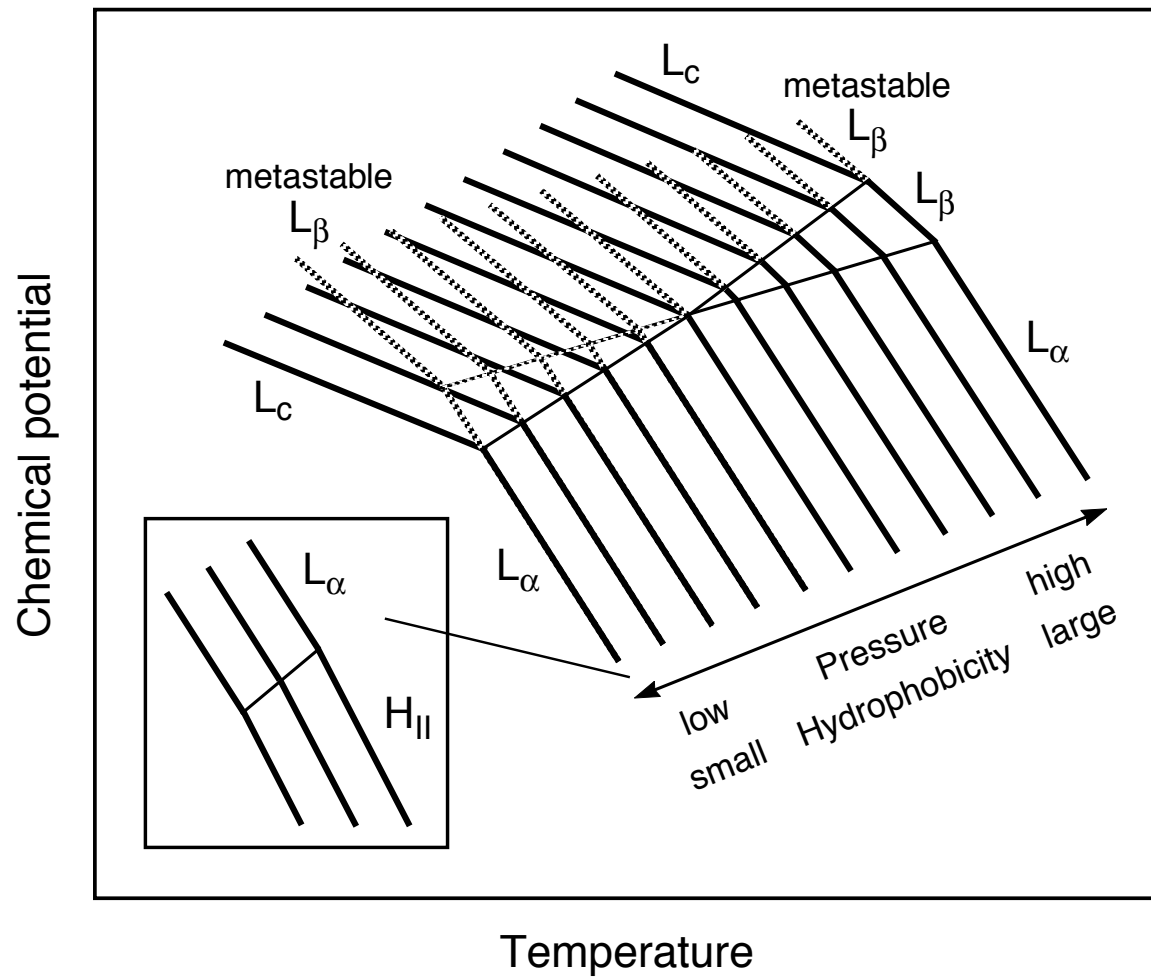


Fig. 8. Matsuki, et al.

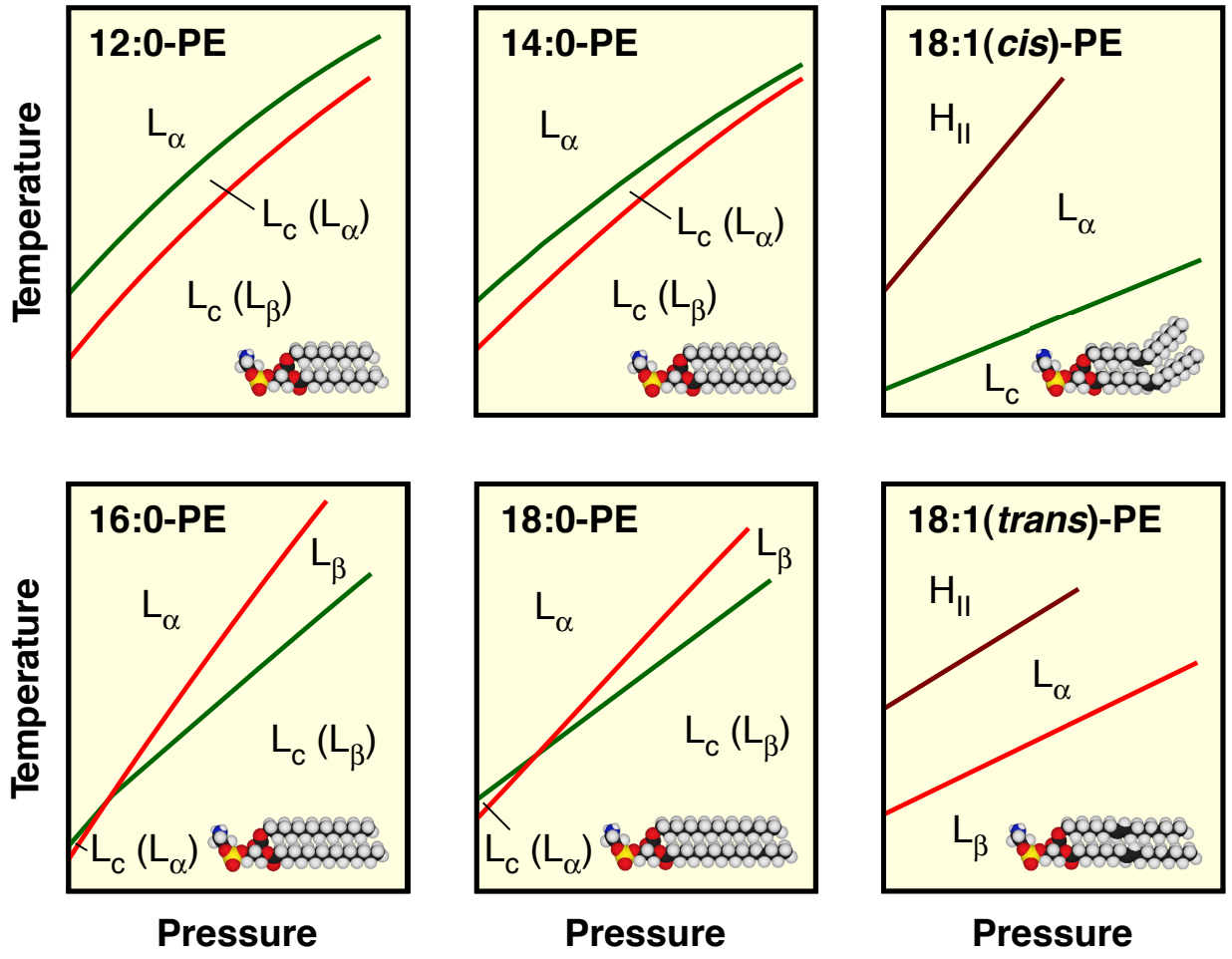


Table 1. Thermodynamic properties for the phase transitions of saturated PE bilayer membranes

Lipid	Transition	$T$ (K)	$T$ (°C)	$dT/dP$ (K MPa <sup>-1</sup> )	$\Delta H$ (kJ mol <sup>-1</sup> )	$\Delta S$ (J K <sup>-1</sup> mol <sup>-1</sup> )	$\Delta V$ (cm <sup>3</sup> mol <sup>-1</sup> )
12:0-PE	L <sub>β</sub> /L <sub>α</sub>	304.1	30.9	0.232	19.9	57	15.2
	L <sub>c</sub> /L <sub>α</sub>	317.5	44.3	0.212	75.3	237	50.3
14:0-PE	L <sub>β</sub> /L <sub>α</sub>	323.0	49.8	0.251	25.1	78	19.5
	L <sub>c</sub> /L <sub>α</sub>	330.1	56.9	0.223	80.8	245	54.5
16:0-PE	L <sub>β</sub> /L <sub>α</sub>	336.7	63.5	0.252	34.7	103	26.0
	L <sub>c</sub> /L <sub>α</sub>	338.5	65.3	0.210	91.2	269	56.6
	L <sub>c</sub> /L <sub>β</sub>	–	–	0.164	–	–	(27.1) <sup>a</sup>
18:0-PE	L <sub>β</sub> /L <sub>α</sub>	347.6	74.4	0.276	39.2	113	31.1
	L <sub>c</sub> /L <sub>α</sub>	348.8	75.6	0.207	102.0	293	60.6
	L <sub>c</sub> /L <sub>β</sub>	–	–	0.180	–	–	(29.5) <sup>a</sup>

<sup>a</sup> The apparent value determined at a high pressure of intersection point.

Table 2. Thermodynamic properties for the phase transitions of unsaturated PE bilayer membranes

Lipid	Transition	$T$ (K)	$T$ (°C)	$dT/dP$ (K MPa <sup>-1</sup> )	$\Delta H$ (kJ mol <sup>-1</sup> )	$\Delta S$ (J K <sup>-1</sup> mol <sup>-1</sup> )	$\Delta V$ (cm <sup>3</sup> mol <sup>-1</sup> )
C18:1( <i>cis</i> )-PE	L <sub>c</sub> /L <sub>α</sub>	267.7	-5.5	0.146	28.0	105	15.3
	L <sub>α</sub> /H <sub>II</sub>	287.7	14.5	0.391	1.4	5	1.9
C18:1( <i>trans</i> )-PE	L <sub>β</sub> /L <sub>α</sub>	311.2	38.0	0.209	33.0	106	22.2
	L <sub>α</sub> /H <sub>II</sub>	337.9	64.7	0.250	2.1	6	1.6

Table 3. Ratios of  $\Delta H$  and  $\Delta V$  between bilayer-nonbilayer and bilayer-bilayer transitions for the unsaturated PE bilayer membranes

Lipid	Ratio of $\Delta H$	Percentage (%)	Ratio of $\Delta V$	Percentage (%)
C18:1( <i>cis</i> )-PE	$\Delta H(L_\alpha/H_{II})/\Delta H(L_c/L_\alpha)$	5.0	$\Delta V(L_\alpha/H_{II})/\Delta V(L_c/L_\alpha)$	12.4
C18:1( <i>trans</i> )-PE	$\Delta H(L_\alpha/H_{II})/\Delta H(L_\beta/L_\alpha)$	6.4	$\Delta V(L_\alpha/H_{II})/\Delta V(L_\beta/L_\alpha)$	7.2

Supplementary Table 1. Thermodynamic properties for the phase transitions of saturated PC bilayer membranes

Lipid	Transition	$T$ (K)	$T$ (°C)	$dT/dP$ (K MPa <sup>-1</sup> )	$\Delta H$ (kJ mol <sup>-1</sup> )	$\Delta S$ (J K <sup>-1</sup> mol <sup>-1</sup> )	$\Delta V$ (cm <sup>3</sup> mol <sup>-1</sup> )
12:0-PC	$L_c/L_x$ <sup>a</sup>	274.9	1.7	0.120	32.9	120	14.0
	$L_x/L_\alpha$ <sup>a</sup>	277.7	4.5	0.150	1.5	5	0.8
	$P_\beta'/L_\alpha$	270.9	-2.3	0.200	7.5	28	5.5
14:0-PC	$L_c/P_\beta'$	290.3	17.1	0.080	25.7	89	7.1
	$L_\beta'/P_\beta'$	288.1	14.9	0.130	4.5	16	2.0
	$P_\beta'/L_\alpha$	297.2	24.0	0.210	25.7	87	18.3
16:0-PC	$L_c/L_\beta'$	294.7	21.5	0.180	26.3	89	16.1
	$L_\beta'/P_\beta'$	307.5	34.3	0.130	4.6	15	1.9
	$P_\beta'/L_\alpha$	315.2	42.0	0.220	36.4	115	25.4
18:0-PC	$L_c/L_\beta'$	304.2	31.0	0.220	28.6	94	20.7
	$L_\beta'/P_\beta'$	324.1	50.9	0.140	5.0	15	2.2
	$P_\beta'/L_\alpha$	328.8	55.6	0.230	45.2	137	31.6

<sup>a</sup> Values in 50% ethylene glycol solution.



Supplementary Table 2. Thermodynamic properties for the phase transitions of unsaturated PC bilayer membranes

Lipid	Transition	$T$ (K)	$T$ (°C)	$dT/dP$ (K MPa <sup>-1</sup> )	$\Delta H$ (kJ mol <sup>-1</sup> )	$\Delta S$ (J K <sup>-1</sup> mol <sup>-1</sup> )	$\Delta V$ (cm <sup>3</sup> mol <sup>-1</sup> )
C18:1( <i>cis</i> )-PC	L <sub>β</sub> /L <sub>α</sub>	232.9	-40.3	0.233	–	–	–
	L <sub>c</sub> /L <sub>α</sub>	256.0	-17.2	0.131	29.4	115	15.1
C18:1( <i>trans</i> )-PC	L <sub>c</sub> /L <sub>β</sub>	282.2	9.0	0.108	35.9	127	13.7
	L <sub>β</sub> /L <sub>α</sub>	284.3	11.1	0.180	23.3	82	14.7